AD-A058 826 PENNSYLVANIA STATE UNIV UNIVERSITY PARK APPLIED RESE--ETC F/G 13/11
INJECTION NOZZLE GEOMETRIES PURSUANT TO THE REDUCTION OF DRAFT --ETC(U)
JUN 78 T A SEYBERT N00017-73-C-1418
UNCLASSIFIED TM-78-172 NL

1 OF 1
AD A058 826

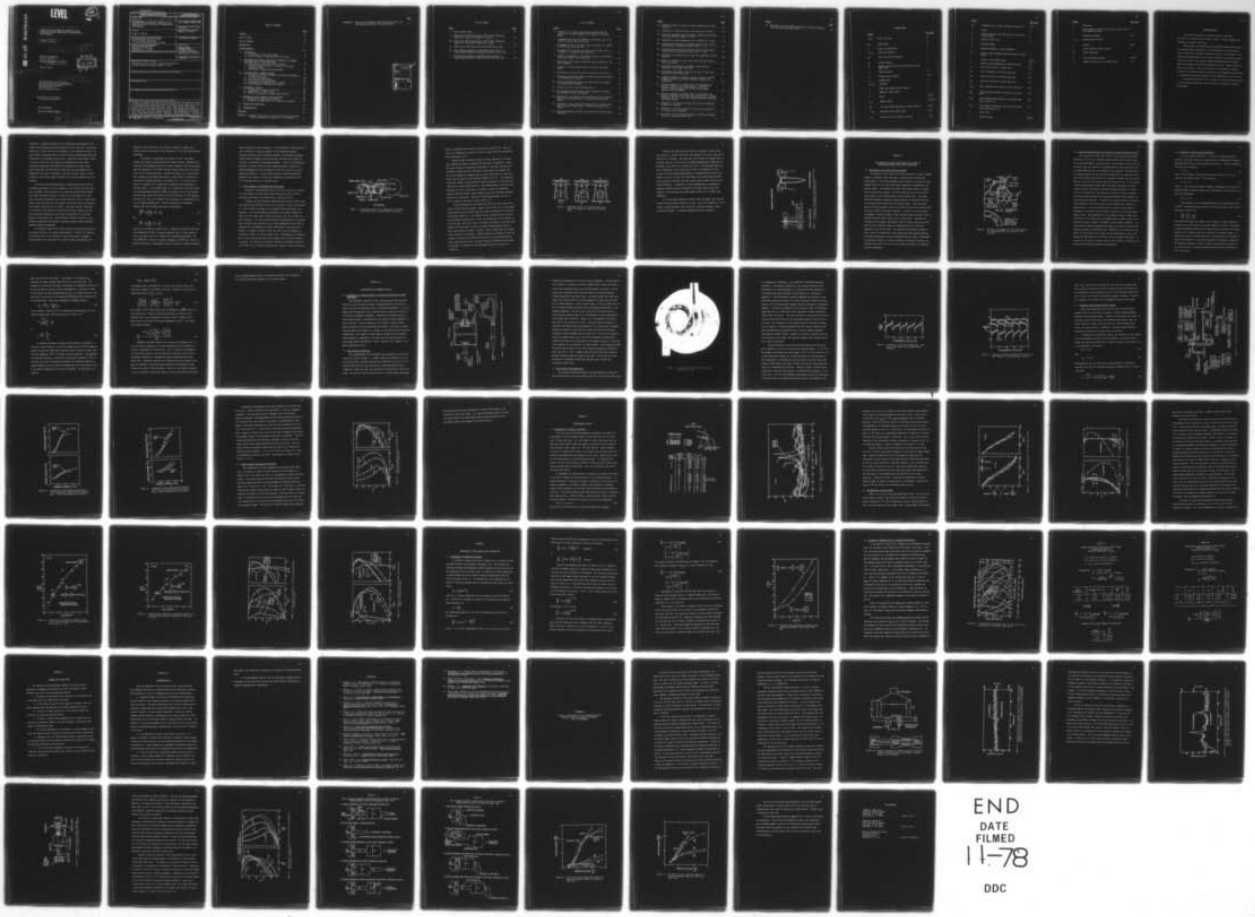

END
DATE FILMED
11-78
DDC

(6) INJECTION NOZZLE GEOMETRIES PURSUANT TO THE REDUCTION OF DRAFT TUBE SURGE IN HYDROELECTRIC PUMP-TURBINES

(10) Thomas A./Seybert

(11) 1 Jun 78 (12) 94p

Technical Memorandum
File No. TM 78-172
June 1, 1978
Contract No. (15) N00017-73-C-1418

Copy No. 12

(14) TM-78-172

(9) Masters thesis

The Pennsylvania State University
Institute for Science and Engineering
APPLIED RESEARCH LABORATORY
Post Office Box 30
State College, PA 16801

Approved for public release
Distribution unlimited

NAVY DEPARTMENT

NAVAL SEA SYSTEMS COMMAND

UNCLASSIFIED

SECURITY CLASSIFICATION OF THIS PAGE (When Data Entered)

REPORT DOCUMENTATION PAGE

READ INSTRUCTIONS BEFORE COMPLETING FORM

1. REPORT NUMBER: TM 78-172

2. GOVT ACCESSION NO.

3. RECIPIENT'S CATALOG NUMBER

4. TITLE (and Subtitle): INJECTION NOZZLE GEOMETRIES PURSUANT TO THE REDUCTION OF DRAFT TUBE SURGE IN HYDROELECTRIC PUMP-TURBINES

5. TYPE OF REPORT & PERIOD COVERED: M.S. Thesis, August 1978

6. PERFORMING ORG. REPORT NUMBER: TM 78-172

7. AUTHOR(s): Thomas A. Seybert

8. CONTRACT OR GRANT NUMBER(s): N00017-73-C-1418

9. PERFORMING ORGANIZATION NAME AND ADDRESS:
The Pennsylvania State University
Applied Research Laboratory
P. O. Box 30, State College, PA 16801

10. PROGRAM ELEMENT, PROJECT, TASK AREA & WORK UNIT NUMBERS

11. CONTROLLING OFFICE NAME AND ADDRESS:
Naval Sea Systems Command
Department of the Navy
Washington, D. C. 20362

12. REPORT DATE: June 1, 1978

13. NUMBER OF PAGES: 94 pages & figures

14. MONITORING AGENCY NAME & ADDRESS (if different from Controlling Office)

15. SECURITY CLASS. (of this report): Unclassified, Unlimited

15a. DECLASSIFICATION/DOWNGRADING SCHEDULE

16. DISTRIBUTION STATEMENT (of this Report)

Approved for public release, distribution unlimited,
per NSSC (Naval Sea Systems Command), 7/5/78

17. DISTRIBUTION STATEMENT (of the abstract entered in Block 20, if different from Report)

18. SUPPLEMENTARY NOTES

19. KEY WORDS (Continue on reverse side if necessary and identify by block number)

20. ABSTRACT (Continue on reverse side if necessary and identify by block number)

A method to eliminate draft tube surge in pump-turbines is proposed by injecting some high energy fluid from the spiral casing into the draft tube counter to the direction of the swirling flow. An air flow facility was used to simulate the rotating flow in the draft tube. This thesis is the result of an investigation of the effectiveness of various nozzle geometries in reducing draft tube surge for given surging conditions. The minimum ratio of bypass flow to draft tube flow required to eliminate surge is determined. The results of these tests provide basic design criteria for selecting injection nozzle configuration.

DD FORM 1 JAN 73 1473 EDITION OF 1 NOV 65 IS OBSOLETE

UNCLASSIFIED

SECURITY CLASSIFICATION OF THIS PAGE (When Data Entered)

TABLE OF CONTENTS

Page

LIST OF TABLES

LIST OF FIGURES

Figure

Page

NOMENCLATURE

Symbol		MLT Units
A, A_3	draft tube area	L^2
A_N	nozzle area	L^2
B	depth of wicket gates	L
D, D_3	draft tube diameter	L
D_2	draft tube throat diameter	L
D'	nozzle diameter	L
$\overline{D}$	diameter associated with the mean area of the draft tube	L
f	surge frequency	$1/T$
g	gravitational constant	L/T^2
H	turbine head	L
K_1, K_2	constants	-
L	draft tube length, nozzle length	L
N	number of wicket gates	-
P	power	ML^2/T^3
P_{11}	specific power	$M/L^{3/2}T^3$
$\overline{\Delta P}$	root mean square amplitude of surge pressure	M/LT^2
Q, Q_T	discharge rate in draft tube	L^3/T
Q_B	discharge rate of injection nozzles	L^3/T

Symbol		MLT Units
Q_T^*	discharge rate in draft tube which occurs at S^*	L^3/T
r	radius	L
r_i	radius from draft tube centerline to wicket gate trailing edge	L
r_w	radius of draft tube	L
R_e	Reynolds number	-
S	momentum parameter or swirl parameter	-
S^*	critical swirl parameter where inception of surge occurs	-
T	torque of the turbine runner	ML^2/T^2
V	velocity vector magnitude at wicket gate exit	L/T
V_A	local axial velocity in draft tube	L/T
V_θ	local rotational velocity in draft tube	L/T
V_R	radial velocity at the wicket gate exit	L/T
V_{θ_i}	rotational velocity at wicket gate exit	L/T
$\overline{V}_{A_T}$	mass averaged axial velocity in the draft tube	L/T
$\overline{V}_{\theta_T}$	mass averaged rotational velocity in the draft tube	L/T
$\overline{V}_{A_T}^*$	mass averaged axial velocity in the draft tube which occurs at S^*	L/T
$\overline{V}_{\theta_T}^*$	mass averaged tangential velocity in the draft tube which occurs at S^*	L/T
W	nozzle width	L
γ	specific weight	M/L^2T^2

Symbol		MLT Units
η	efficiency	-
θ	angle between a radial line and the velocity vector V at wicket gate exit	-
ν	kinematic viscosity	L^2/T
π_1, π_2	dimensionless functions	-
ρ	density	M/L^3
ϕ	nozzle injection angle (Table I)	-
ϕ_2	speed coefficient	-
Ω	flux of angular momentum	ML^2/T^2
ω	angular velocity of the turbine runner	$1/T$

ACKNOWLEDGEMENTS

The author would like to thank his thesis co-advisers, Mr. Walter S. Gearhart and Dr. Joseph R. Reed, for their guidance and assistance throughout this study.

This research was performed at the Garfield Thomas Water Tunnel of the Applied Research Laboratory of The Pennsylvania State University under contract with the Naval Sea Systems Command, and sponsored by the United States Department of the Interior, Bureau of Reclamation, Denver, Colorado, as part of the Bureau's Pumped Storage Research Activities under their Energy Research and Development Program. Special thanks is given to Dr. Henry T. Falvey of the Bureau of Reclamation at Denver, Colorado, who provided frequent consultation and implemented the exchange of information and hardware required in the completion of this research.

The author would also like to thank all of the Water Tunnel personnel who helped him with this project but are too numerous to mention individually.

CHAPTER I

INTRODUCTION

1.1 Description of Draft Tube Surge

During the past decade, considerable attention has been directed toward the production of energy by pollution-free methods. As a result of this interest, emphasis has been placed on the development of high head pump-turbine units because of their production of relatively inexpensive energy. Pump-turbines in general are used to satisfy peak power requirements using the pump-storage concept. Because of the high variability of required power production of a peaking power plant, pump-turbines are required to run over a wide range of operating conditions. A phenomenon called draft tube surge is associated with hydroelectric turbines and pump-turbines which operate at off design conditions. Draft tube surge is a hydrodynamic instability which occurs as a result of excess rotation remaining in the water as it leaves the turbine runner and enters the draft tube. Figure 1 is a schematic of a turbine cross section. Due to the excess rotation, a swirling flow (axial motion and rotational motion at the same time) is established in the draft tube of the turbine. When the flux of angular momentum entering the draft tube becomes sufficiently large compared to the flux of linear momentum in the draft tube, a reversal of flow direction occurs along the draft tube centerline. In the field of fluid machinery this condition is known as inception of draft tube surge. A rope-like helical vortex develops around the region of reversed flow and precesses about the draft tube

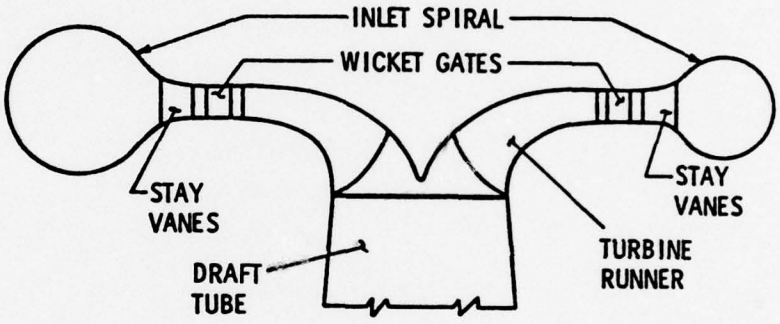

Figure 1. Schematic of a turbine cross section illustrating the geometry of the flow passage in the region of the wicket gates.

centerline. Cassidy and Falvey [2] reported that the presence of the helical vortex produced unsteady pressures in the draft tube. Falvey and Cassidy [4] later observed the frequency of the unsteady pressure to be very regular, indicating that the helical vortex precessed about the tube centerline at a reasonably regular rate. Along with this periodic vibration in the draft tube, the surges are responsible for many other undesirable operating characteristics in hydroelectric power plants. These undesirable characteristics, which may occur individually or in combination, are noise, vibrations, variation in power output, vertical movement of the turbine runner and shaft, and pressure pulsations in the penstock.

The draft tube surge phenomenon is complicated by many factors, including vaporization of water, geometry of the turbine and draft tube, and the dynamic characteristics of the penstock and electrical network. The vortex core which arises as a result of the swirling flow in the draft tube has been observed to be filled with air, water, or water vapor. Falvey [5] noted that the fluid phase of the vortex core was related to the tailwater elevation of the turbine. For high tailwater elevations, the vortex core was observed to be filled with water, whereas for the lower tailwater elevations, water vapor and sometimes air was found present in the vortex core. The two-phase flow which occurred for low tailwater conditions was observed to produce pressure surges which were somewhat reduced in magnitude.

The geometric shape of the draft tube has also been observed to be a governing influence on surging characteristics. Palde [9] conducted an extensive study on the influence of draft tube shape on surging characteristics and found that, for a given turbine installation, the

geometry of the draft tube could affect the range of surging, the frequency band of the surge, and the amplitude of the resulting pressure pulsations.

In an effort to coordinate the studies of draft tube surge, attempts were made to develop predictive terms of surge. Murakami [8] noted that the frequency and force of surge vibrations could be predicted when the dimensions of the draft tube and turbine runner and load conditions of the turbine were known. Cassidy and Falvey [2] later showed that frequency and pressure pulsations of surge could be correlated to the amount of angular momentum in the draft tube. In a later paper by Falvey and Cassidy [4], dimensionless parameters were developed to describe surge. It was assumed that, for a particular draft tube shape, the root-mean-square amplitude $\left(\overline{\Delta P}\right)$ and frequency (f) of the unsteady pressure surge are both functions of the fluid density (ρ) and kinematic viscosity (ν), draft tube diameter (D) and length (L), discharge (Q) and flux of angular momentum (Ω). Standard techniques of dimensional analysis gave the following functional relationships:

$$\frac{D^4\overline{\Delta P}}{\rho Q^2} = \pi_1\left(\frac{\Omega D}{\rho Q^2}, \frac{L}{D}, R_e\right) \tag{1}$$

and

$$\frac{fD^3}{Q} = \pi_2\left(\frac{\Omega D}{\rho Q^2}, \frac{L}{D}, R_e\right) \quad , \tag{2}$$

where R_e is the Reynolds number $4Q/\pi D\nu$. Inspection of $\Omega D/\rho Q^2$ shows that this represents the ratio of angular momentum flux to linear momentum flux in the draft tube and is defined as the momentum parameter. The ratio $D^4\overline{\Delta P}/\rho Q^2$ is called the pressure parameter, and fD^3/Q is called the frequency parameter. Experimental studies proved that a high correlation

exists between all three parameters. For any hydraulic turbine installation, relations of pressure parameter versus momentum parameter, frequency parameter versus momentum parameter, and frequency parameter versus pressure parameter can be developed, provided that a method is available to determine the momentum parameter. Palde [10] developed a graphical technique called the swirl momentum method to predict the momentum parameter and the occurrence of draft tube surge for a given wicket gate geometry. A more accurate means of predicting momentum parameter with respect to wicket gate opening was developed by Yocum [17] through the use of a computer model.

1.2 Prior Attempts to Eliminate Draft Tube Surge

Because of the detrimental effect draft tube surge has on hydraulic power plants, various attempts have been made over the years to alleviate the problem, some dating back to 1880 and earlier.

Probably the most frequently mentioned method used to reduce draft tube surge is the admission of air into the runner or draft tube (Figure 2). Both location and manner of air injection have been found to be important. Air has been admitted upstream of the runner, between the runner and the wicket gates, through the runner core, and through the draft tube wall. For low tailwater elevation installations, the pressure near the draft tube centerline is less than atmospheric and all that is necessary for air admission is proper ventilation to the vortex core. However, for higher tailwater levels, the use of an air compressor is necessary to inject air into the draft tube. Consequently, air admission may be costly because the most severe surging occurs at high tailwater elevations. Air admission was found to reduce the pressure fluctuation in the draft tube of several installations. However, other installations

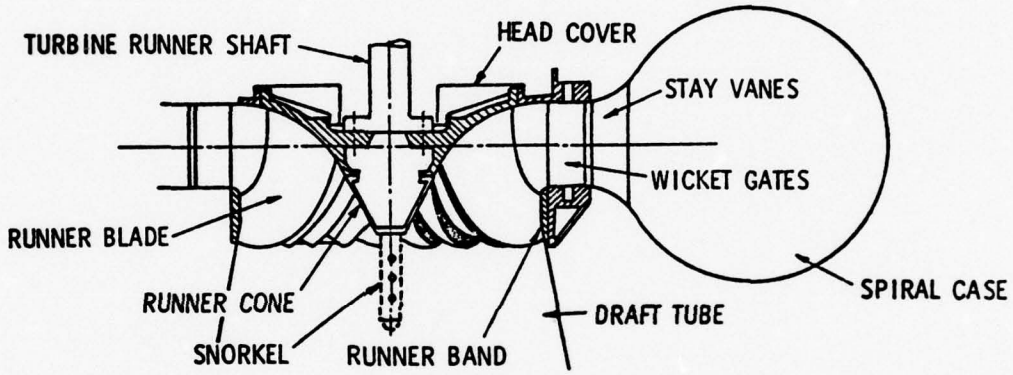

Figure 2. Arrangement used for air admission to the draft tube in an effort to reduce draft tube surge.

using air admission have reported an increase in surge [5]. This is due to the dependence of surge on cavitation number which was observed by Gerich and Raabe [6].

Because surge is caused by excess rotation remaining in the flow after leaving the runner, attempts have been made to eliminate or reduce the excess rotation by placing fins parallel to the draft tube axis and attached to either the draft tube wall or the runner core (Figure 3A). If the fins extend far enough across the draft tube throat to touch each other, they are know as flow splitters (Figure 3B) [5]. Fin geometries varying the number of fins along with length and depth of fins have been tried, but all with limited success. The disadvantages of fins and flow splitters are loss in efficiency, necessity to guard the appentures against cavitation damage, high frequency noise, and structural problems involved in installation. Because of these disadvantages, the use of fins is normally restricted to small units [5].

Other investigations with model test facilities have shown that a hollow cylinder which resembles a barrel with the ends cut out and placed concentrically with the draft tube will reduce the amplitude of the pressure surges (Figure 3C). The coaxial hollow cylinder has been noted to reduce pressure pulsations up to 70%. By placing the hollow cylinder in the draft tube, the vortex core is coaxially contained in the draft tube. Falvey [5] noted that a vortex core which forms coaxially with the draft tube produces no surge. However, a major problem with the coaxial hollow cylinder is structural. Supports which are necessary to keep the cylinder centered in the draft tube would have to be strong enough to resist large lateral forces, yet small enough to minimize flow blockage. The problem of cavitation of the appendages would also have to be considered.

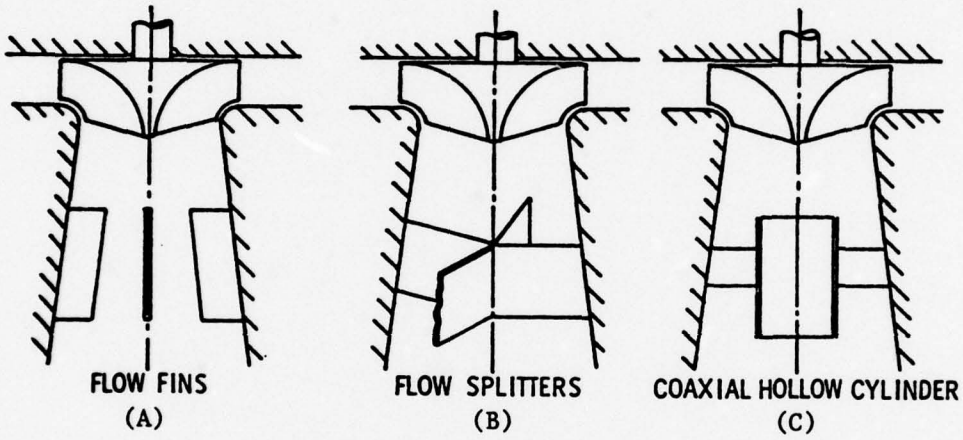

Figure 3. Appendages placed in the draft tube in an effort to contain or reduce the rotational flow.

Probably the oldest approach used in an attempt to reduce draft tube surge is to replace the vortex core present in the draft tube with a solid body of rotation. The solid body can be either an integral part of the draft tube as in the case of the Moody Spreading Cone (Figure 4A) or attached to the runner core (Figure 4B) [5]. The reasoning behind the use of extensions to the runner core is that the elimination of the reverse flow area reduces unsteadiness by streamlining the overall flow. However, the use of runner core extensions allows unfavorable velocity head recovery in the draft tube and produces high lateral forces on the runner extension. In addition to these disadvantages, an adjustable diameter extension would be necessary for optimal results since the diameter of the reverse flow region varies from 0.2 to 0.8 draft tube diameters.

Of all the above methods to reduce draft tube surge, only limited success has been obtained with any of them. Each of the methods, to some degree, causes efficiency loss, results in cavitation damage, induces structural problems, or requires expensive auxiliary equipment.

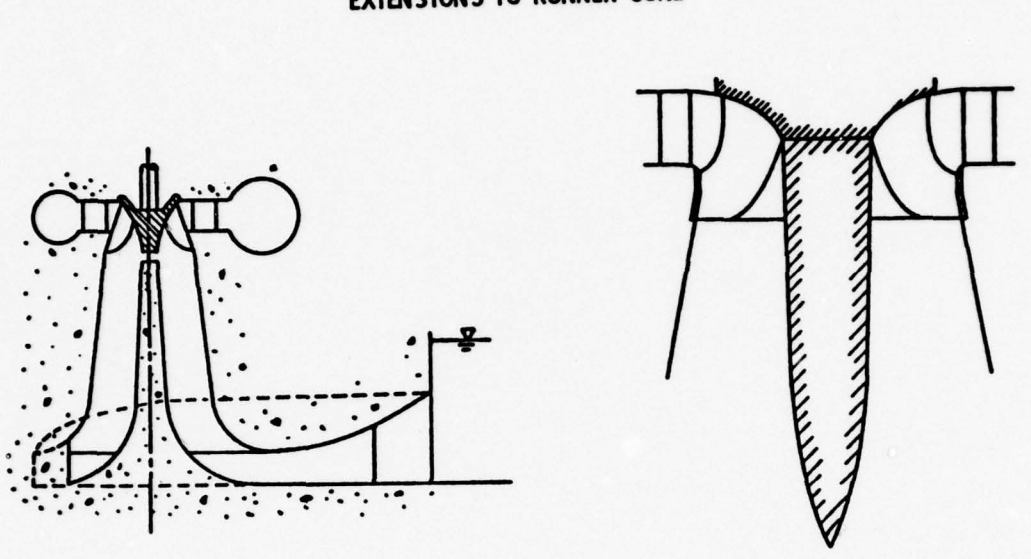

Figure 4. Extensions to the runner core placed in the draft tube in an effort to streamline draft tube flow.

CHAPTER II

THE REDUCTION OF DRAFT TUBE SURGE BY INJECTION OF COUNTER ROTATIONAL FLUID IN THE DRAFT TUBE

2.1 Description of the Fluid Injection Method

The subject of this thesis is directly related to a newly proposed method to eliminate draft tube surge in hydroelectric turbines and pump-turbines. The method considered here consists of a series of flush-mounted nozzles in the draft tube placed immediately downstream of the turbine runner. The nozzles will inject high energy fluid in a peripheral direction with respect to the draft tube axis and into the draft tube counter to the rotating motion of the swirling flow. The intent behind this method is momentum exchange between the injected fluid and the swirling fluid exiting from the turbine runner. With the proper amount of fluid injection, swirl in the draft tube could be reduced below the point of draft tube surge inception. A schematic of the proposed arrangement is shown in Figure 5 where the high energy injection fluid is bypassed from the spiral casing at the turbine inlet. Although not indicated in the figure, two separate rows of nozzles could be provided with one row of nozzles capable of injecting fluid in a direction opposite to that of the other. The reduction of positive or negative swirl, which is encountered at below design and above design operating conditions respectively, would be possible with this type of arrangement. An appropriate system of valving activated on the basis of wicket gate opening could control the flow to the nozzles and control the number of nozzles discharging.

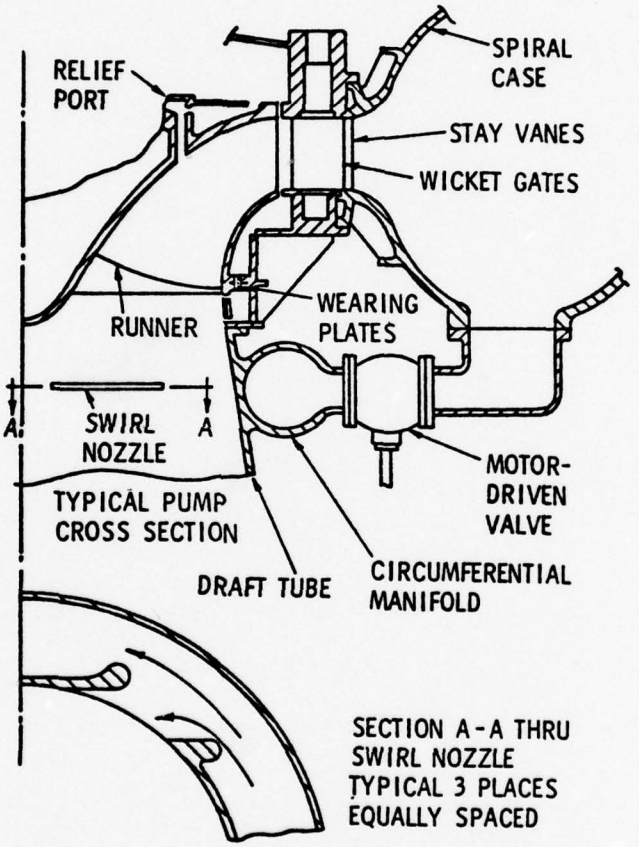

Figure 5. Schematic arrangement of the proposed method of eliminating draft tube surge by fluid injection.

2.2 Desirable Characteristics of Injection of Counter Rotational Fluid

The reduction of draft tube surge by fluid injection has several advantages over the other methods which have been used to reduce surge. In the proposed method, the nozzles will be flush-mounted on the wall of the draft tube and, therefore, a minimum amount of flow disturbance will be present when the use of the nozzles is not required. The presence of the nozzles should not cause any loss in efficiency or cavitation resistance of the machine when there is no injection, provided that cavitation does not occur in the slots when the jets are not in use. As the turbine operates progressively further away from design conditions, the swirl nozzles could be activated to provide an increasing amount of counter-swirl to the draft tube. By using such a system, an infinite number of off design conditions which are encountered during turbine shutdown and start-up could be handled. A second row of nozzles capable of injecting fluid opposite to that of the other row would permit the reduction of negative swirl. Also, this system will not require the placement of appendages in the draft tube that will be subject to fluctuating hydrodynamic loads. The feasibility of this proposal, however, hinges upon the amount of fluid which must be bypassed from the spiral casing to the injection nozzles in order to eliminate a given surging condition. Any fluid which is bypassed represents an energy loss across the machine and therefore produces an efficiency loss. Therefore, an evaluation of the amount of fluid which must be drawn from the high pressure side of the turbine and discharged into the draft tube is of primary importance. An estimate of the ratio of bypassed flow to flow through the turbine can be obtained on the basis of momentum considerations.

2.3 Prediction of Bypass Flow Requirements

For any turbine installation, the amount of angular momentum present in the draft tube can be expressed by the dimensionless momentum parameter $\Omega D/\rho Q^2$ for any given operating condition. The basic expression for power can be shown as

$$P = \omega T \quad , \tag{3}$$

where ω is the angular velocity of the turbine runner, and T is the torque of the turbine runner. The expression

$$T = \Omega_1 - \Omega_2 \quad , \tag{4}$$

where $\Omega_1 - \Omega_2$ is the rate change of moment of momentum of the fluid as it passes through the turbine runner can be substituted into Equation (3) to obtain the expression

$$\frac{P}{\omega} = \Omega_1 - \Omega_2 \quad . \tag{5}$$

This equation can be nondimensionalized by multiplying both sides by $D/\rho Q^2$. Rearranging terms, Equation (5) takes the form of the equation obtained by Palde [13]:

$$\frac{\Omega_2 D}{\rho Q^2} = \frac{\Omega_1 D}{\rho Q^2} - \frac{PD}{\rho \omega Q^2} \quad . \tag{6}$$

This expression shows very simply that the amount of angular momentum present in the draft tube for any given condition is equal to the amount of angular momentum induced by the turbine wicket gates minus the torque imparted to the turbine runner and converted to mechanical energy. To maximize the effect of fluid injection on surge reduction, the amount of bypass fluid required to eliminate surge must be minimized. Therefore, the momentum parameter of a given surging condition must be reduced to the critical value of momentum parameter which describes inception of draft tube surge.

The momentum parameter or swirl parameter shall be defined as S, where

$$S = \frac{\Omega D}{\rho Q^2} \tag{7}$$

The relative influence of the various operating characteristics of the turbine with respect to swirl parameter becomes more apparent if the swirl parameter can be expressed as a ratio of angular velocity to axial velocity in the draft tube. Figure 6 illustrates the nomenclature and stations considered. From Figure 6, the draft tube flow (Q) and flux of angular momentum (Ω) can be determined at the exit of the wicket gates (WG) as

$$Q = \int_{WG} V_R dA = V_R 2\pi r_i B \tag{8}$$

and

$$\Omega = \rho \int_{WG} V_R \left(r_i V_{\theta_i} \right) dA = \rho Q r_i V_{\theta_i} \tag{9}$$

where B is the wicket gate depth, and V_{θ_i} is the rotational component of velocity at the wicket gate exit. Substitution of Equation (9) into Equation (7) yields:

$$S = \frac{\rho Q r_i V_{\theta_i} D}{\rho Q^2} = \frac{r_i V_{\theta_i} D}{Q} \quad , \tag{10}$$

where D is the draft tube diameter. The presence of a given amount of swirl in the draft tube above the point of inception of surge will generate a pressure pulsation of some prescribed frequency. The swirl in the draft tube shall be generated by a set of wicket gates as indicated by Figure 6. Conservation of momentum is assumed between the wicket

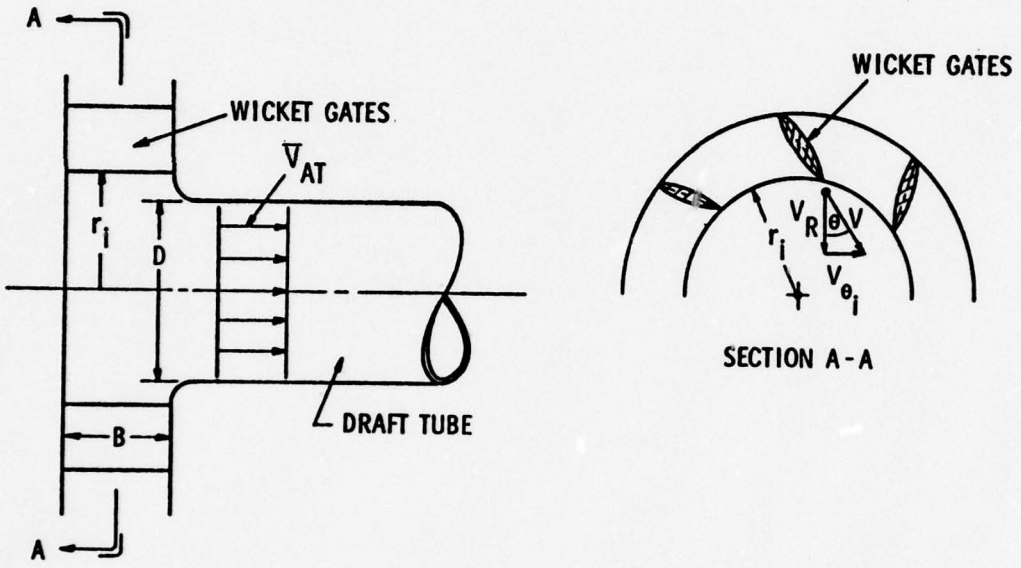

Figure 6. Nomenclature and stations considered in the analysis of the swirl parameter.

gates and the draft tube throat. From Figure 6, the quantity $\overline{V}_{A_T}$ represents the mass averaged axial velocity in the draft tube. The assumption is made that the radial distribution of tangential velocity at a given section in the draft tube is represented by a potential vortex. On this basis, the mass averaged quantity $\overline{V}_{\theta_T}$, at a given section of the draft tube, would occur at the diameter $\overline{D}$ associated with the mean area of the draft tube. This can be expressed in algebraic form as

$$r_i V_{\theta_i} = \frac{\overline{D}}{2} \overline{V}_{\theta_T} = \frac{D}{2\sqrt{2}} \overline{V}_{\theta_T} \quad . \tag{11}$$

If the results of Equation (11) are substituted into Equation (10), the relation between swirl and velocity ratio is found to be

$$S = \frac{D^2 \overline{V}_{\theta_T}}{2\sqrt{2}\, \overline{V}_{A_T}} \cdot \frac{4}{\pi D^2}$$

or

$$S = \frac{\sqrt{2}}{\pi} \cdot \frac{\overline{V}_{\theta_T}}{\overline{V}_{A_T}} \quad . \tag{12}$$

To evaluate the amount of bypass fluid required to eliminate a particular surge condition, it shall be assumed that the swirl parameter present in the draft tube before injection will be reduced to some critical swirl parameter $\left(S^*\right)$ (* denotes critical condition). The quantity of bleed flow required to obtain the critical swirl parameter $\left(S^*\right)$ in the draft tube can be evaluated by equating the difference between the angular momentum from the turbine discharge and that of the bypass fluid to the angular momentum at the critical condition. On this basis, the relation

$$Q_T \bar{V}_{\theta_T} - Q_B \bar{V}_B = Q_T^* \bar{V}_{\theta_T}^* \tag{13}$$

is obtained, where the subscript T refers to the turbine throat, and subscript B refers to the bypass fluid flow. Equation (13) can be non-dimensionalized by $Q_T^* V_{A_T}^*$ to give:

$$\frac{\left(Q_T \bar{V}_{\theta_T}\right)}{\left(Q_T^* \bar{V}_{A_T}^*\right)} - \frac{\left(Q_B \bar{V}_B\right)}{\left(Q_T^* \bar{V}_{A_T}^*\right)} = \frac{\left(Q_T^* \bar{V}_{\theta_T}^*\right)}{\left(Q_T^* \bar{V}_{A_T}^*\right)} = \frac{\pi}{\sqrt{2}} S^* \tag{14}$$

The velocity of the bleed fluid V_B can be expressed as $\sqrt{2gH}$, where H is the turbine head. Using the continuity principle and Equation (12), Equation (14) can be rearranged to provide a ratio of bypass flow to draft tube flow in terms of the swirl parameters S and S^*. The predictive equation becomes:

$$\frac{Q_B}{Q_T} = \frac{2.22\ \bar{V}_{A_T}^* \left[S\left(\frac{\bar{V}_{A_T}}{\bar{V}_{A_T}^*}\right) - S^*\left(\frac{\bar{V}_{A_T}^*}{\bar{V}_{A_T}}\right)\right]}{2gH} \quad . \tag{15}$$

Examining the above equation for a given swirl parameter (S), it is seen that the numerator of the above expression will be essentially constant, independent of turbine head. This is based on the assumption, for cavitation purposes, that the velocity in the draft tube throat at the design condition for conventional turbine installations has some upper limit. Therefore, Equation (15) indicates that the required ratio Q_B/Q_T to eliminate a particular swirl parameter (S) decreases as some reciprocal function as head increases. Since the ratio Q_B/Q_T represents a loss in efficiency, this would indicate that the decrease in efficiency,

due to bleeding bypass fluid to the injection nozzles, will be smaller for a high head turbine compared to a low head turbine.

CHAPTER III

INJECTION NOZZLE GEOMETRY STUDIES

3.1 Optimization of Nozzle Geometry for Effective Reduction of Draft Tube Surge

The successful reduction of draft tube surge by fluid injection depends upon the efficient exchange of momentum between the injection nozzle flow and the rotational flow of the swirling condition. It would appear that the geometry of the injection nozzle would have an effect on the efficient exchange of momentum. Therefore an extensive series of tests were performed to determine the most effective nozzle geometry for fluid injection. Various geometries with different length-to-width ratios along with circular geometries were tested. The effect of fluid injection angle with respect to a tangent to the draft tube wall was also investigated. The results of these studies indicate that the optimum nozzle geometry is dependent on the head and flow characteristics of a given pump-turbine installation. Table I (page 37) is a summary of the nozzle geometries tested.

3.2 Test Facility Description

The investigations for this thesis were conducted in an air flow facility as shown in Figure 7. Studies conducted by Cassidy [1] and Palde [9] using a similar facility have shown that the use of air as a working fluid has been quite successful in characterizing the swirl parameter in draft tube flow and predicting the occurrence of draft tube surge. The main air supply was provided by a variable speed centrifugal

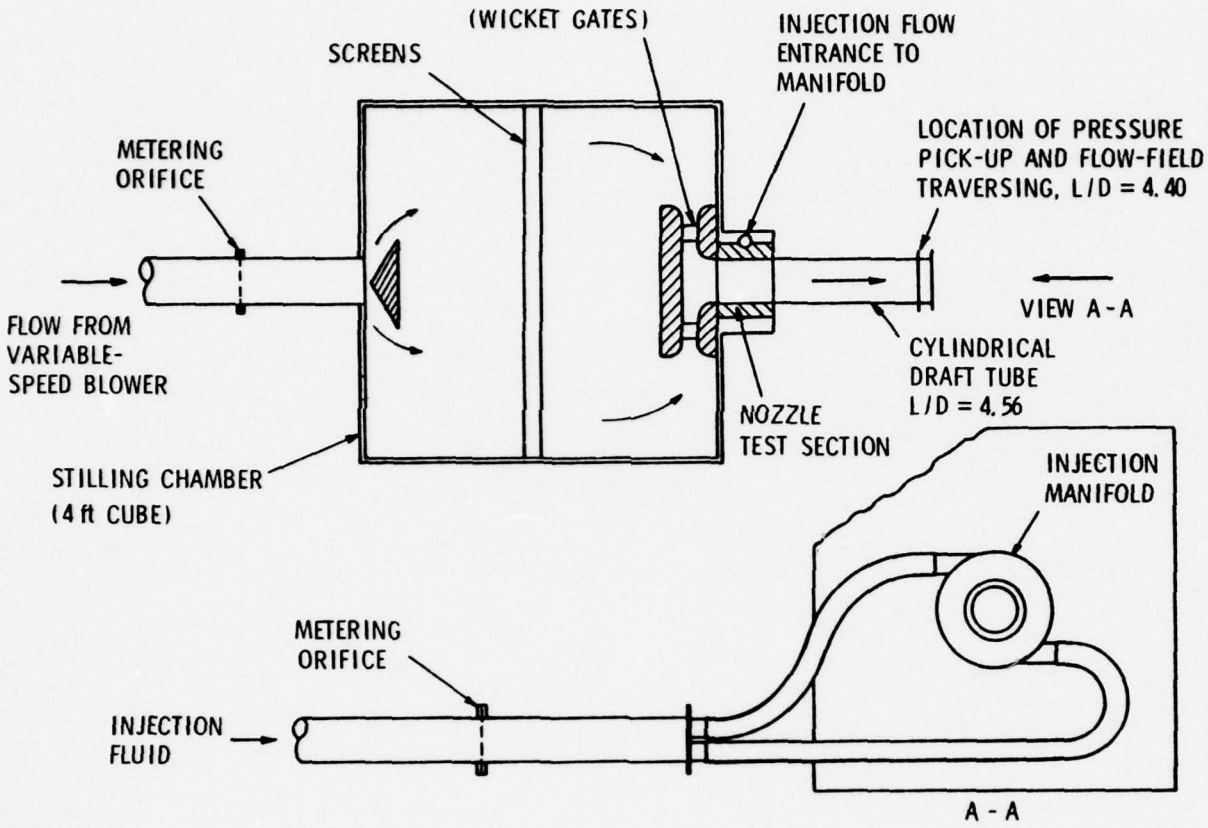

Figure 7. Schematic of test facility used in the draft tube surge study.

blower and was measured by an orifice meter arrangement. The metered air was diffused as it entered a stilling chamber where screens were used to reduce flow turbulence across the stilling chamber flow field. The air entered the cylindrical draft tube and nozzle test section radially through wicket gate type swirl vanes. The angle between the vanes and a radial line could be set at any value between 0^{o} (radial position) and 82.5^{o} (closed position). Later in this thesis, it will be shown that the air flow angle through the wicket gates is directly proportional to the momentum parameter. The nozzle test section provided three points of fluid injection equally spaced in a circumferential plane perpendicular to the draft tube centerline. Figure 8 is a photograph of the nozzle test section with nozzle #5 in place. Injection fluid provided by an auxiliary centrifugal blower and measured by an orifice meter arrangement entered the manifold of the injection nozzle test section and passed through the nozzle openings into the draft tube. Any ratio of injection fluid flow (bypass flow) (Q_B) to fluid flow through the wicket gates (turbine flow) (Q_T) could be provided by the proper setting of a butterfly valve connected to the auxiliary air supply blower. After passing through the nozzle test section, the air flow continued through the cylindrical draft tube (L/D = 4.56). Pressure taps and probe holes were located at various locations along the length of the tube. The studies were conducted with a cylindrical draft tube and also with an elbow type (Fontenelle) draft tube.

3.3 Test Facility Instrumentation

The unsteady pressure produced by the swirling flow in the draft tube was monitored at the last pressure tap (L/D = 4.40) on the draft tube

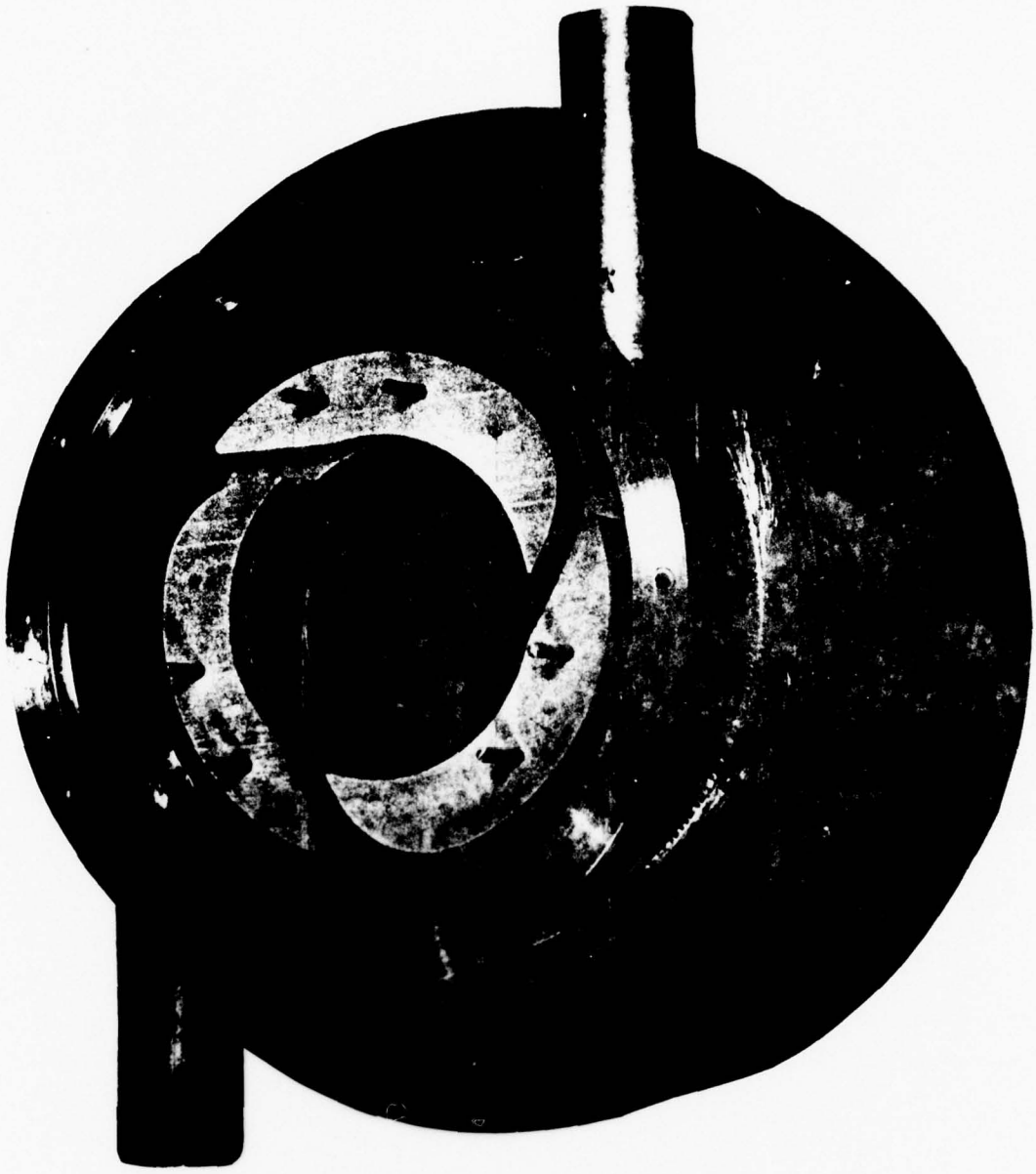

Figure 8. Photograph of Nozzle Test Section with nozzle #5 in place.

by a dynamically calibrated 1 psi (0.689N/cm^2) differential pressure transducer. The dynamic calibration of the pressure transducer was performed by Dr. Frank Archibald of the Applied Research Laboratory of The Pennsylvania State University as described by Dr. Archibald in Appendix A. The differential pressure transducer was connected to the draft tube pressure tap with a 4" (10 cm) long piece of surgical tubing having a 1/4" (6.35 mm) inside diameter and was referenced to atmospheric pressure. To obtain the magnitude of the pressure surge, the transducer signal was sent to a DISA (Type 55 D35) RMS meter through a Krohn-Hite (Model 3342) line filter. The line filter had a characteristic 48 dB per octave rolloff and was set to pass everything between 20 and 120 Hz for all tests. The frequency of the pressure surge was obtained by passing the raw signal to a Spectral Dynamics Real Time Analyzer (Model SD-301) which was operated in conjunction with a Spectral Dynamics Ensemble Averaging Unit (Model SD-302). Knowing the pressure surge RMS value and the frequency of the surge, both pressure parameter and frequency parameter could be calculated.

Velocity profiles in the draft tube and behind the wicket gates were obtained by the use of two three-hole pressure probes. A 1/8" (3.18 mm) diameter prism probe was used through a 3/16" (4.76 mm) wide arc slot in the wicket gate assembly for traversing across the trailing edge of the wicket gates to determine the velocity profile and fluid flow angle. Figure 9 shows typical flow angle variation behind the wicket gates with respect to circumferential location. Similarly, Figure 10 shows typical variations of velocity with respect to circumferential location. In the draft tube, a 1/4" (6.35 mm) diameter wedge probe was used to investigate velocity profiles and pressure distributions across the diameter of the

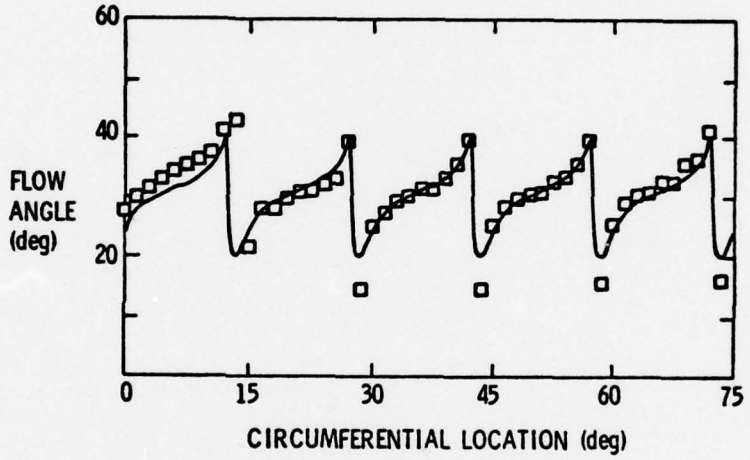

Figure 9. Variation of flow angle behind the wicket gates with respect to circumferential location.

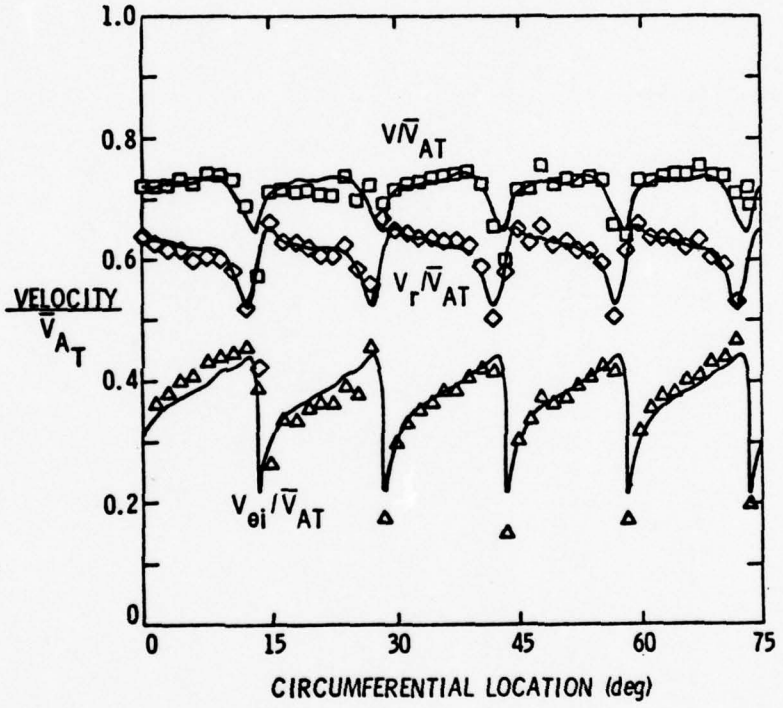

Figure 10. Velocity distribution behind the wicket gates with respect to circumferential location.

draft tube. The probe was inserted into the draft tube through probe holes provided at different locations along the draft tube centerline. Both probes were used in conjunction with a multi-channel scanner valve and a 0.5 psi (0.345 N/cm^2) differential pressure transducer. Figure 11 is a schematic of the draft tube instrumentation used in the study.

3.4 Preliminary Data Required Before Testing

Before any significant data could be taken, the wicket gate assembly had to be calibrated to produce a relation between momentum parameter and wicket gate angle. Instead of using wicket gate angle, an arbitrary linear scale was used to determine gate opening. When the wicket gates were closed, the scale read 0.0. When the gates were radial, the scale read 9.5. Therefore, a relation between momentum parameter and wicket gate setting could be developed.

To simplify the calibration process, the relation for swirl parameter as described by Equation (10) was examined. The angle between a radial line and the velocity vector V shown in Figure 6 was defined to be θ, and therefore, from Figure 6:

$$V_R = V \cos \theta \tag{16}$$

and

$$V_{\theta_i} = V \sin \theta \quad . \tag{17}$$

Using Equation (8), the relation for volume flow rate, along with Equations (16) and (17) and substituting into Equation (10), it could be shown that

$$S = \frac{r_i V_{\theta_i} D}{Q} = \frac{r_i \, V \sin \theta \, D}{r_i \, V \cos \theta \, 2\pi B} = \frac{\tan \theta \, D}{2\pi B} \quad . \tag{18}$$

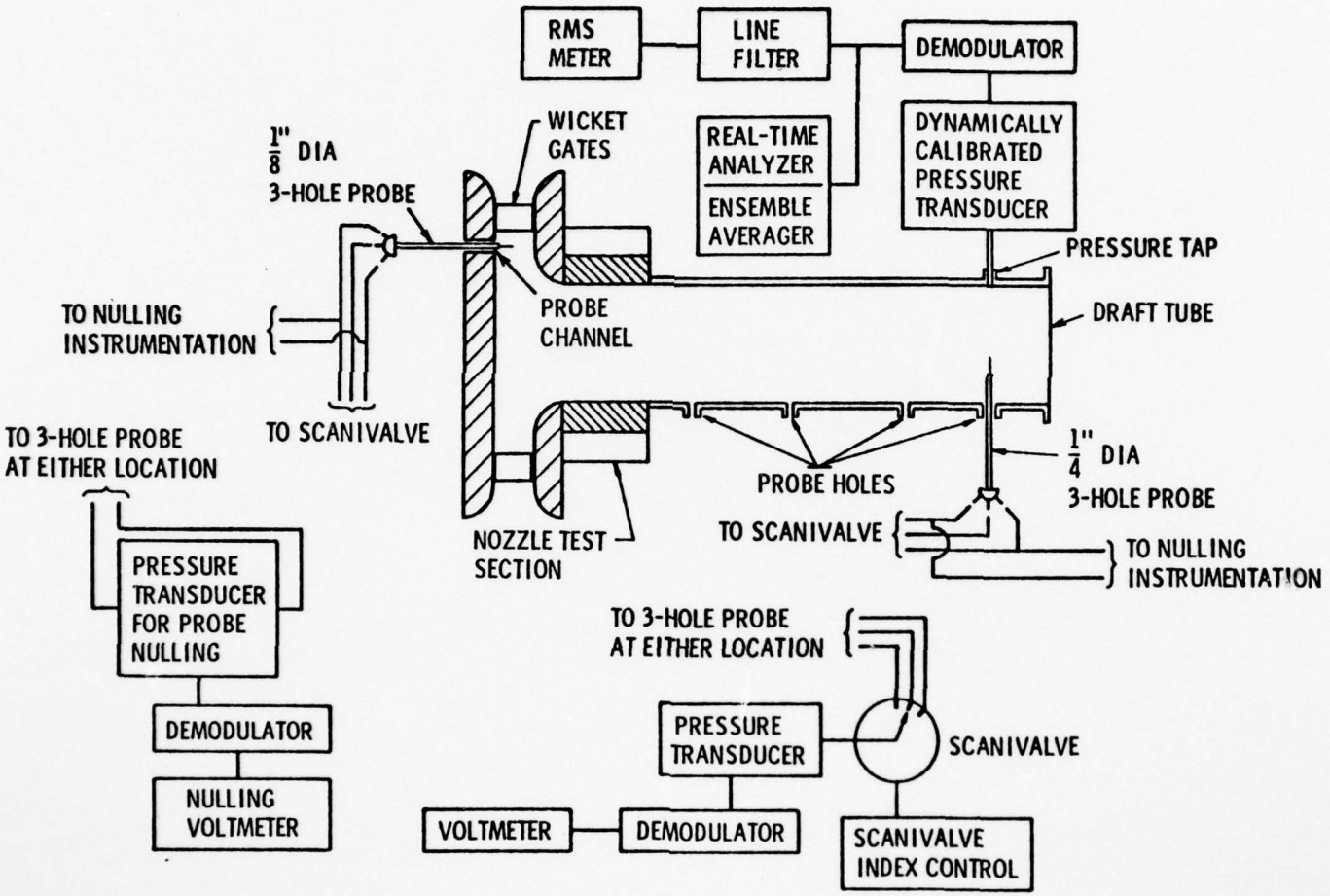

Figure 11. Schematic of draft tube instrumentation.

For the test facility, the values of D and B indicated by Figure 6 were known constants. Equation (18), therefore, could be reduced to

$$S = K_1 \tan \theta \quad , \tag{19}$$

where $K_1 = 0.557$. Equation (19) shows that momentum parameter (swirl parameter) is only a function of fluid flow angle at the wicket gate trailing edge for the test facility. To calibrate the wicket gate assembly, a series of measurements were taken across the wicket gates trailing edge at various wicket gate settings. The arithmetic mean flow angle was determined across five wicket gates (75 data points) for each wicket gate setting. With this information, a relation between swirl parameter and wicket gate setting was developed and is shown in Figure 12. It was also necessary to determine the relations of pressure parameter and frequency parameter as functions of momentum parameter for the particular test facility. Palde [9] reported the effect of draft tube shape upon surging characteristics and, therefore, a separate set of relations had to be developed for both the cylindrical and elbow type draft tubes. For various momentum parameters, the RMS value and frequency of the pressure surge were determined by the instrumentation described earlier. From this data, the necessary relations could be developed. Since the test facility used for this study was very similar to that used by Palde [9], it was desirable to get similar relations of pressure parameter and frequency parameter as a function of momentum parameter. Figures 13 and 14 show the relations obtained in this study for the cylindrical and elbow type draft tubes, respectively. On the same figures, Palde's data are plotted to show that the data are in fairly good agreement with the previously determined relations.

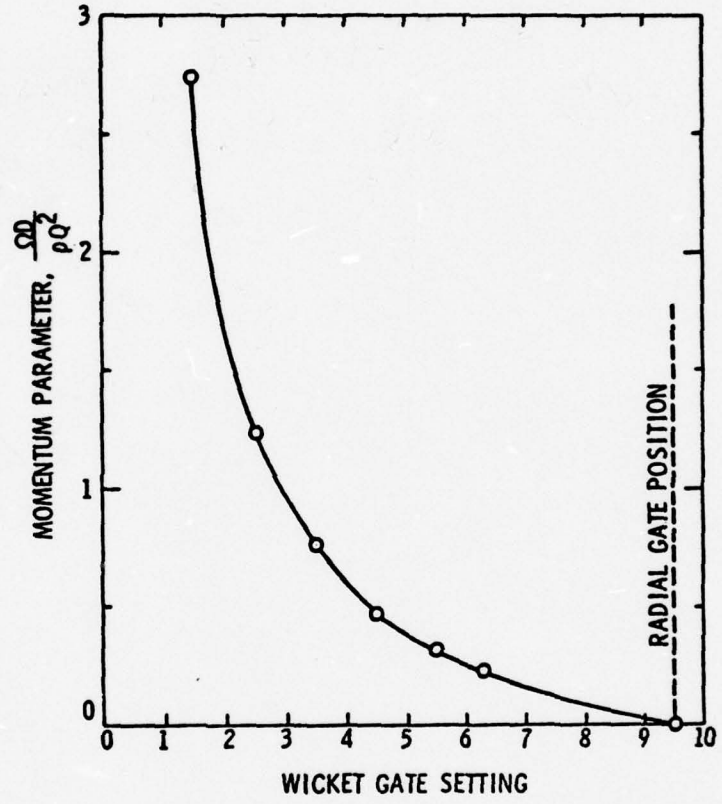

Figure 12. The developed relation between swirl parameter and wicket gate setting for the test facility.

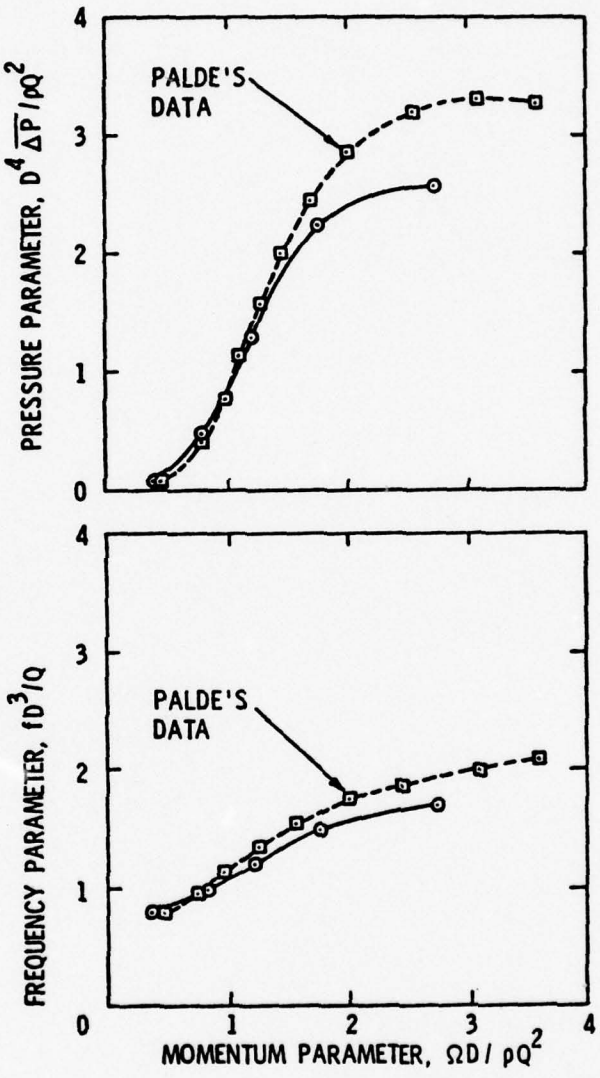

Figure 13. Comparison of the surging characteristics of the cylindrical draft tube with Palde's data. Circles show present test results.

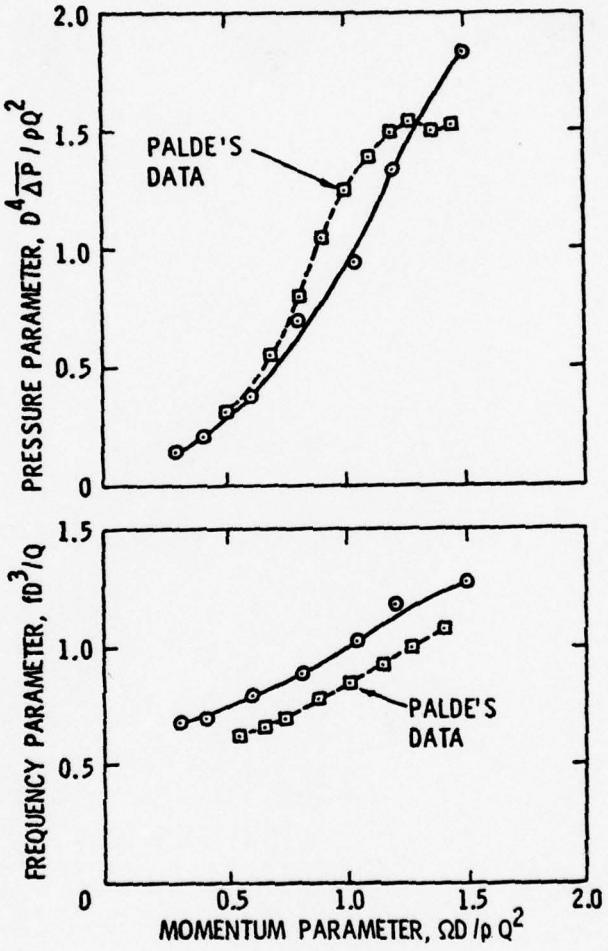

Figure 14. Comparison of the surging characteristics of the elbow type draft tube with Palde's data. Circles show present test results.

Preliminary investigations were also performed in the draft tube flow field. Velocity profiles were developed for a series of momentum parameters. Both the axial velocity component and the rotational velocity component, nondimensionalized by the mass average axial velocity in the draft tube, were plotted as functions of nondimensional radius. Figure 15 shows the characteristic curves for swirl parameters of 0.24, 0.41, 0.80, and 1.18. It can be seen in the axial velocity distribution that a region of reverse flow occurs for all swirl parameters and becomes increasingly larger as swirl parameter increases in magnitude. The axial velocity distributions also approach a potential vortex at the outer region and the inner region takes the form of a solid body. The rotational velocity distribution shows that the product $V_\theta r$ increases for increasing swirl parameter. At S = 0.24, there is no surge; yet, there is considerable rotation in the flow. The inception of surge is very close to S = 0.33.

3.5 Nozzle Geometry Optimization Procedure

The optimization of nozzle geometry was performed in two parts. First, the effects of angle of fluid injection (ϕ) with respect to a tangent line to the draft tube wall in a circumferential plane was investigated. The nozzle shape and area were held constant while various injection angles were tested for effectiveness in reducing draft tube surge for S = 0.80 and S = 1.18. The values of S = 0.80 and S = 1.18 were selected for testing because these are values of swirl parameter which are commonly encountered in field installations. From these data, an optimum angle of injection was selected and the remaining series of tests used this optimum angle of injection which investigated the effects of various nozzle geometry shapes. The effects of length-to-width ratio along with

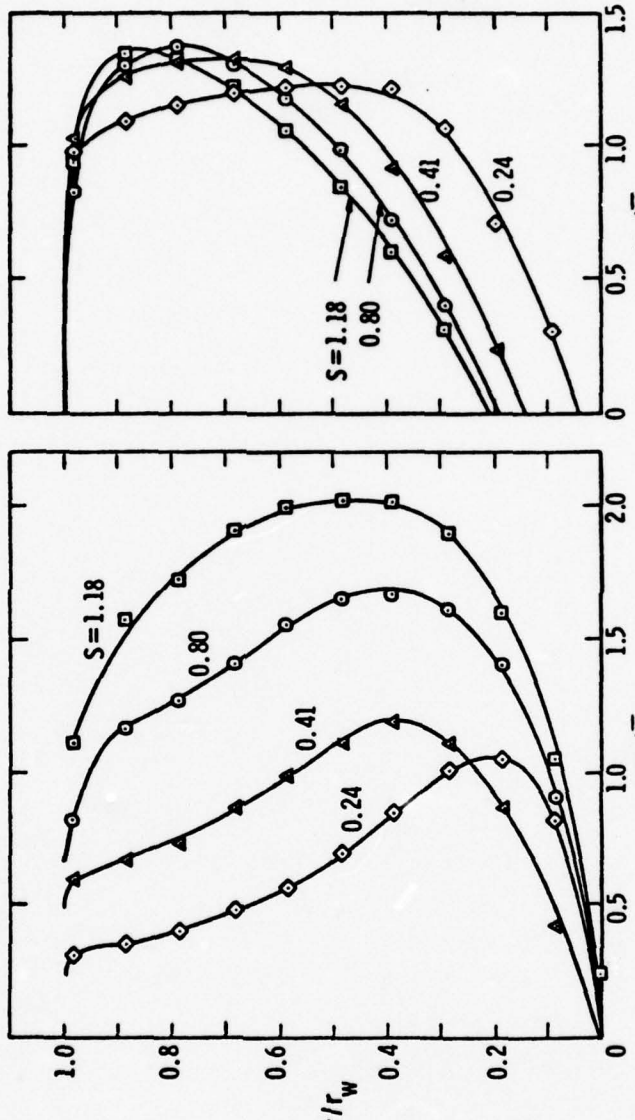

Figure 15. Axial and tangential velocity distribution for various swirl conditions.

varying nozzle area were investigated for their effectiveness in the reduction of draft tube surge. All nozzle optimization tests for injection angle effects and nozzle shape effects were performed with the cylindrical draft tube attached to the test facility.

CHAPTER IV

EXPERIMENTAL RESULTS

4.1 Optimization of Angle of Injection

The first step in the nozzle geometry optimization procedure was to determine the most effective angle of fluid injection for the reduction of draft tube surge. For this series of tests, the nozzle area and shape were held constant while the angle of injection (ϕ) was studied at four different values, namely, 0^{o}, 15^{o}, 30^{o}, and 45^{o}. Table I defines the angle of injection with respect to the draft tube and also lists the various nozzle geometries investigated in this study. Nozzle #5 was used for the optimization of the fluid injection angle. It should also be pointed out that nozzle area A_N in Table I is the sum of all three nozzle areas injecting into the draft tube. Also, A_T is defined as the area of the draft tube throat.

To determine the optimum angle of injection, each angle was studied to see how it affected the characteristics of the surging condition. Of utmost importance is the effect of angle of injection on the reduction of pressure parameter. The amount of bypass fluid required to eliminate surge at swirl parameters of 0.80 and 1.18 was measured for each angle of injection. The Spectral Dynamics Real Time Analyser was used to determine when surge was gone. Figure 16 shows a typical series of plots received from the analyser. Since dBs are related to volts by the expression

$$Volts = -20 \; Lob \; dB \tag{20}$$

and volts are related directly to pressure through the transducer

Table I

NOZZLE SHAPES TESTED

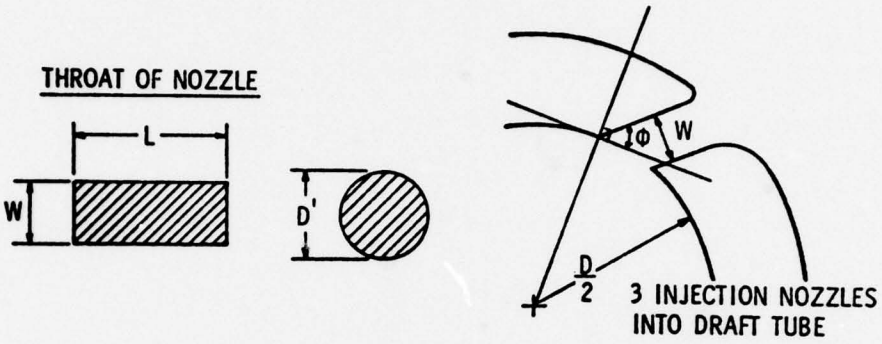

Nozzle Number	Injection Angle, Φ (deg)	Nozzle Area, A_N (sq in.)	A_N/A_T (%)	L/W
1	30	1.500	5.09	8.0
2	↓	0.750	2.54	4.0
3		0.375	1.27	0.5
4	↓	1.125	3.84	1.5
5	0	0.750	2.54	1.0
	15	↓	↓	↓
	30			
	45			
6	30	0.188	0.64	4.0
7	↓	0.750	2.54	0.25
8		0.610	2.04	circle, D' = 0.5 in.
9		1.325	4.48	circle, D' = 0.75 in.
10		0.375	1.27	1.0
11		↓	↓	4.0
12				0.25
13		1.50	5.09	1.0
14	↓	↓	↓	4.0
15				0.25

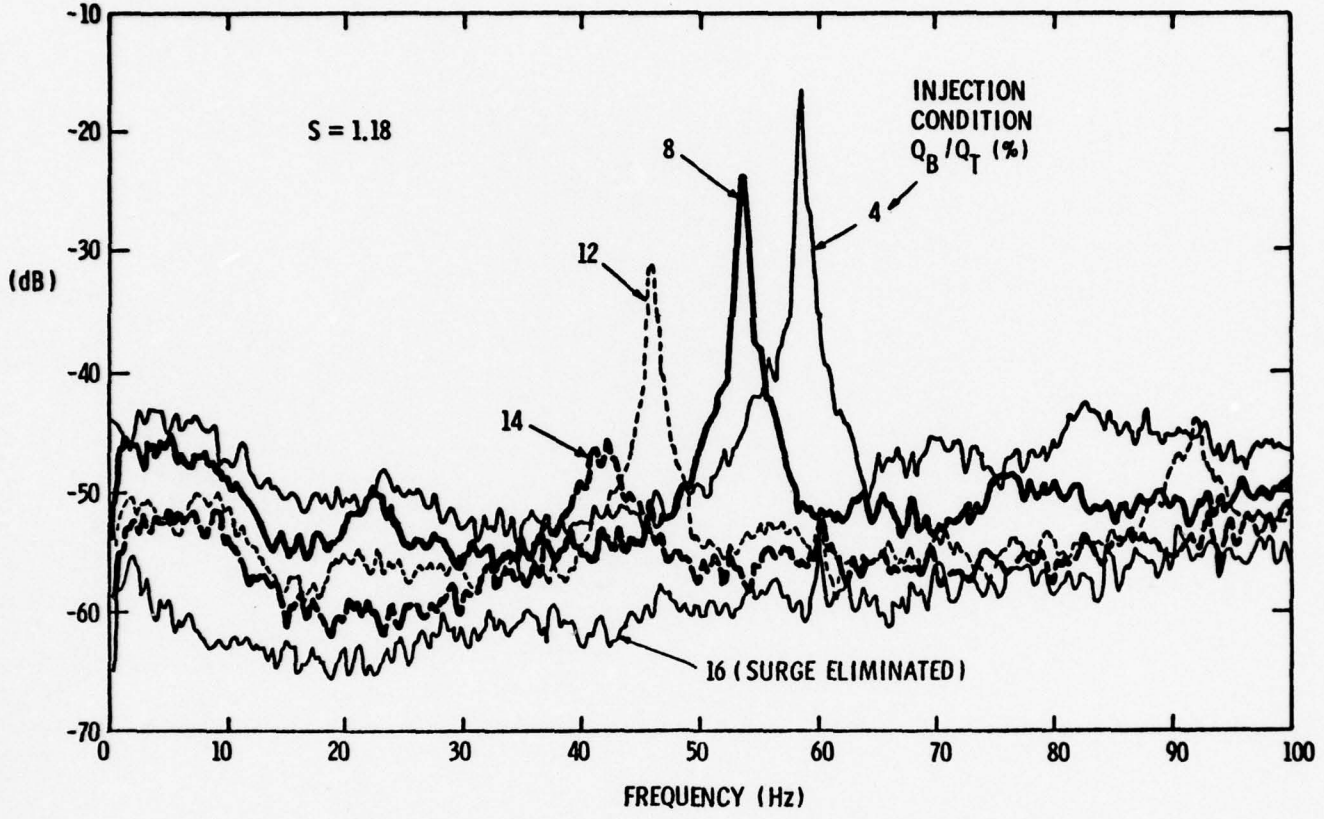

Figure 16. Spectral analysis of surge for various conditions of fluid injection.

constant, it can be seen in Figure 16 that surge pressure was systematically reduced by increasing amounts of injection fluid. Notice that at an injection ratio Q_B/Q_T of 16%, surge disappeared from the analyser spectrum. Figure 17 shows the effect of increasing fluid injection upon the magnitude of the unsteady pressure in the draft tube for all four injection angles at both S = 1.18 and 0.80. The plots show that up to an angle of 45^o, there is no significant difference in reduction of pressure parameter for any given angle of injection. At S = 1.18, the flow ratio required for the elimination of surge is essentially constant at 16% for all injection angles. A similar statement can be made for S = 0.80.

Velocity profiles were also obtained in the draft tube at probe hole L/D = 4.40 for each angle of injection at the point of surge elimination. Figure 18 shows that for the four angles of injection, the rotational velocity profile and the axial velocity profile are essentially the same at these conditions. With this evidence, it was concluded that for an angle of injection up to 45^o, there was no measurable difference in the effective reduction of draft tube surge using nozzle geometry #5. For this study, it was assumed that this was true for all nozzle geometries. However, in order to continue the experiments on nozzle geometry shape, an angle of injection had to be selected. An injection angle of 30^o was used for the remaining series of tests.

4.2 Optimization of Nozzle Shape

Table I is a list of the nozzle geometries tested. The first nine nozzle shapes in Table I were initially studied for area ratio effects. However, nozzles #2, #5, and #7 comprised a series of nozzles where the area ratio was constant and the shape varied. Nozzle shapes 10 through 15

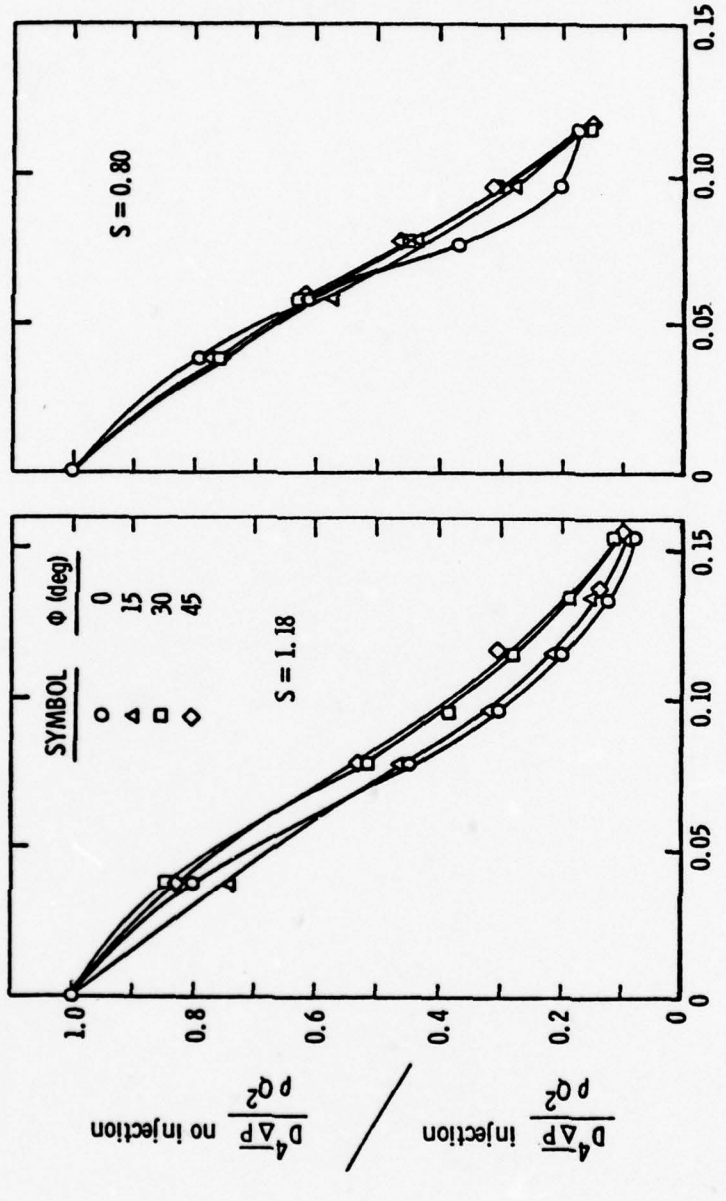

Figure 17. Comparison of injection angle on the reduction of surge.

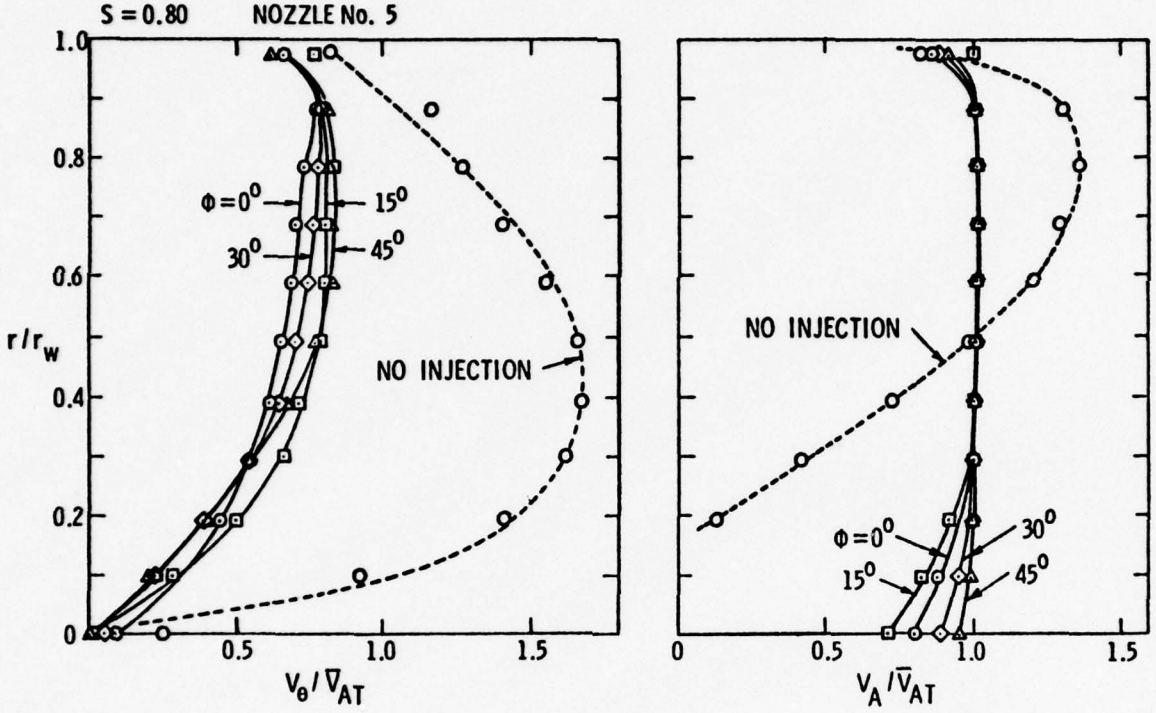

Figure 18. Axial and tangential velocity profiles comparing the effect of nozzle injection angle, S = 0.80.

were used to compliment the study of length-to-width effects upon constant area ratio nozzles.

Each nozzle was placed into the test facility and tested for its effectiveness in the reduction of surge for swirl parameters of 0.80 and 1.18. A nozzle which required less bypass fluid to eliminate surge was declared more efficient than the other. A progressive look at the reduction of surge in terms of pressure parameter with respect to increasing flow ratio was studied for each nozzle. For all cases, an increase in the amount of injected fluid would result in a decrease in the magnitude of the pressure parameter and frequency parameter as earlier illustrated by Figure 16. Figure 19 shows the effect of increasing flow ratio on pressure parameter for swirl conditions of 1.18 and 0.80. The nozzle shapes used in these plots were selected to show the effect of decreasing area ratio on the amount of bypass fluid required to eliminate a given surging condition. The last data point on each curve defines the exact amount of fluid required to eliminate surge for the given nozzle shape. Figure 19 shows that for a given ratio of Q_B/Q_T, the reduction in the surge pressure amplitude is greater as A_N/A_T decreases. This results directly from the fact that to inject a given ratio of Q_B/Q_T into the draft tube, the turbine head and, hence, the nozzle fluid velocity must increase as A_N/A_T decreases. Since the momentum of the injected fluid increases as the square of the spouting velocity from the nozzles, smaller flow ratios are required to eliminate surge as the head of the turbine increases. This was suggested by Equation (15).

The effect of various nozzle length-to-width ratios on surge reduction was studied for area ratios of 1.27, 2.54, and 5.09, all expressed in percent. For a swirl parameter of 1.18 and a constant area

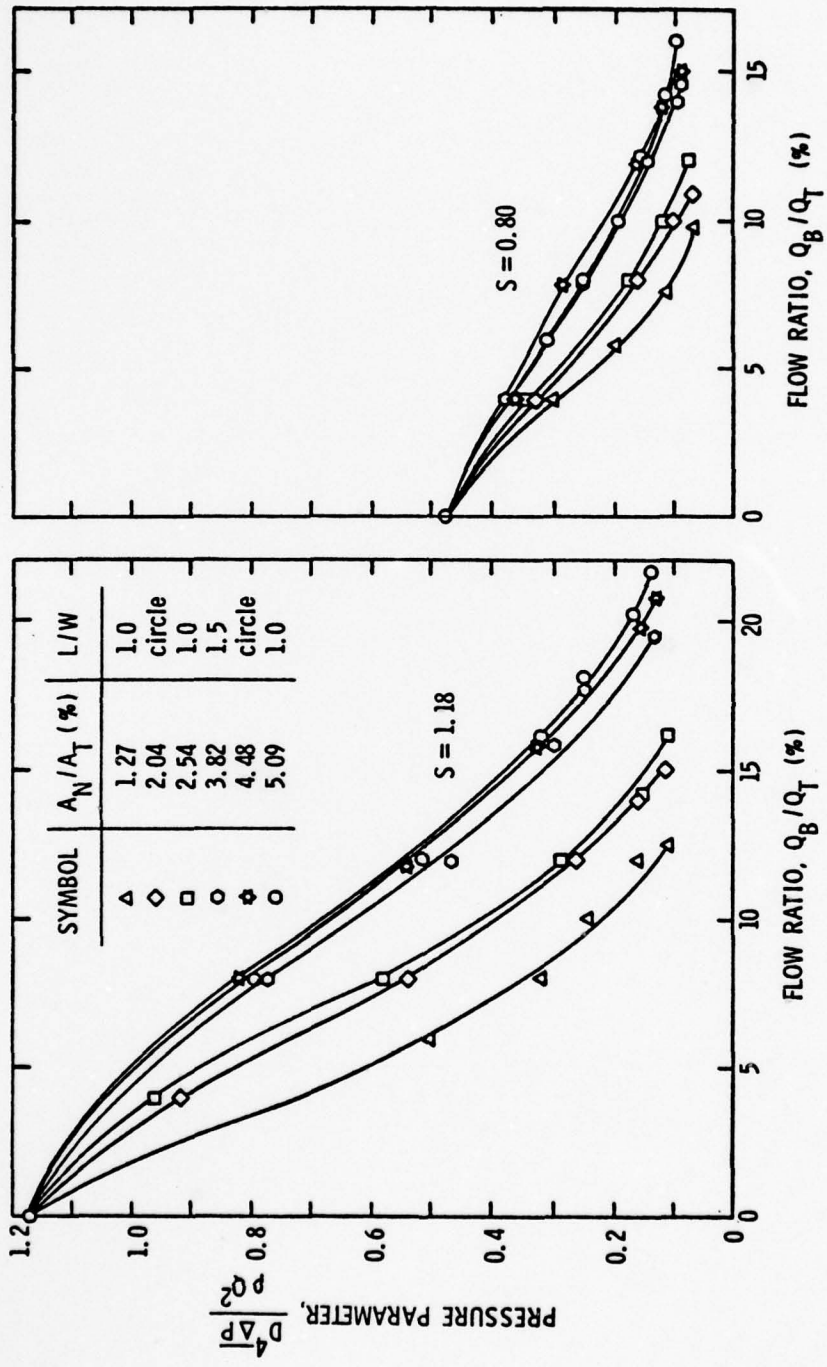

Figure 19. Comparison of nozzle geometries on the reduction of surge.

ratio of 2.54, the amount of bypass fluid required for surge elimination varied from 16.1% to 19.8% with respect to the various length-to-width ratios tested. However, at A_N/A_T = 1.27, the amount of bypass fluid only varied from 12.5% to 14.1%, and at A_N/A_T = 5.09, the variation was even smaller (21.7% to 22.6%). Figure 20 is a plot of flow ratio versus area ratio, which includes the results of all the nozzle shapes tested for S = 1.18. Figure 21 is a similar figure only with S = 0.80. Figures 20 and 21 show that for a constant area ratio of 2.54%, there was an observable difference in the amount of injection fluid required to eliminate surge for various L/W ratios at S = 1.18 and to a lesser degree at S = 0.80. However, at constant area ratios of 1.27% and 5.09% for both S = 1.18 and 0.80, the amount of required injection fluid measured for the various L/W ratios was considered to be within the limits of experimental error. It was further noticed that only nozzle #7 in Figure 20 indicated that variability in length-to-width of a nozzle would cause a significant increase or decrease in effective reduction of surge. Since that data point was only one in twenty examined for L/W effects, it was concluded that no appreciable difference was observed in the ratio of Q_B/Q_T required to eliminate surge at a given A_N/A_T for the various nozzle geometries tested. This result suggests that the choice of nozzle geometry to be used for a given A_N/A_T to eliminate draft tube surge would consist of selecting that geometry which would produce minimum hydraulic losses and permit the easiest fabrication. On this basis, a circular nozzle would seem appropriate.

4.3 Effects of Injection on Surge Characteristics

Figures 16 and 17 were presented to show the effects of injection on pressure parameter and frequency parameter of a given surging

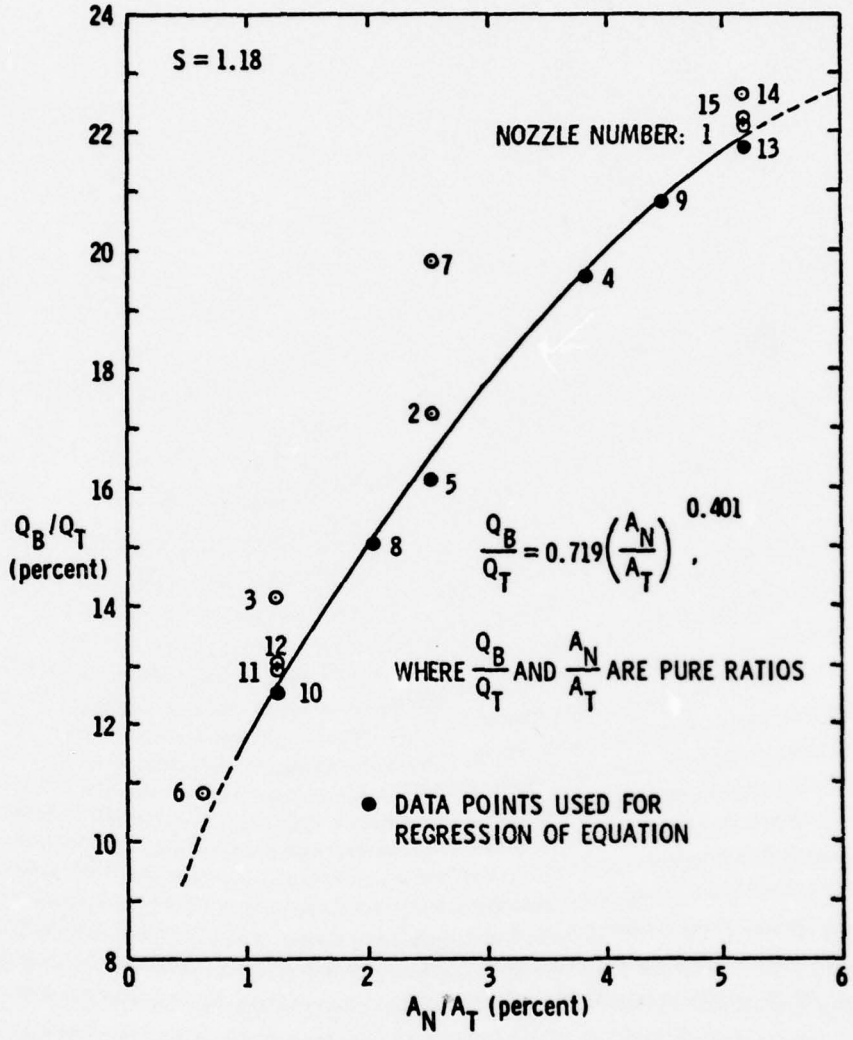

Figure 20. Injection flow required to eliminate surge for all nozzles tested using the cylindrical draft tube, S = 1.18.

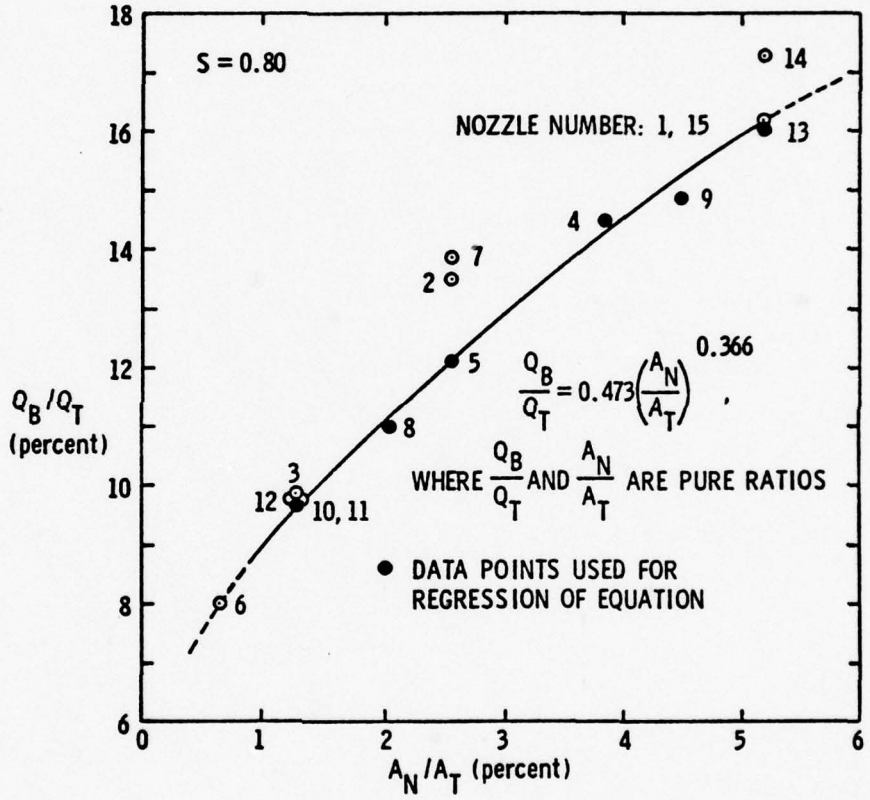

Figure 21. Injection flow required to eliminate surge for all nozzles tested using the cylindrical draft tube, S = 0.80.

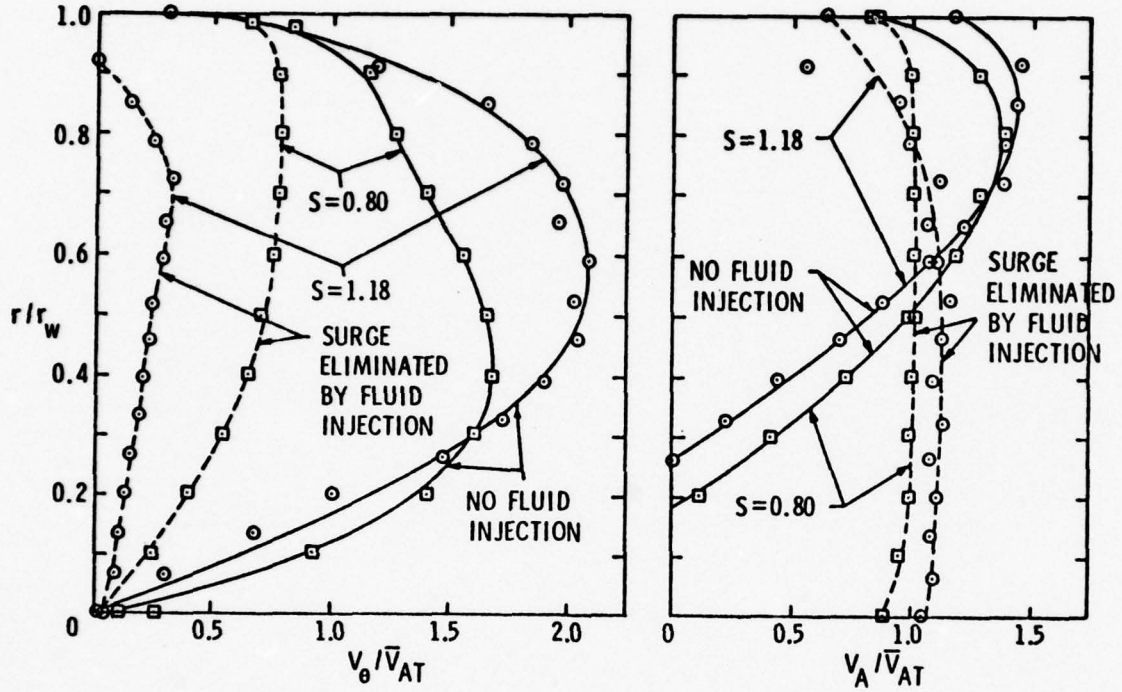

Figure 22. The effect of injection on the axial and tangential velocity profiles.

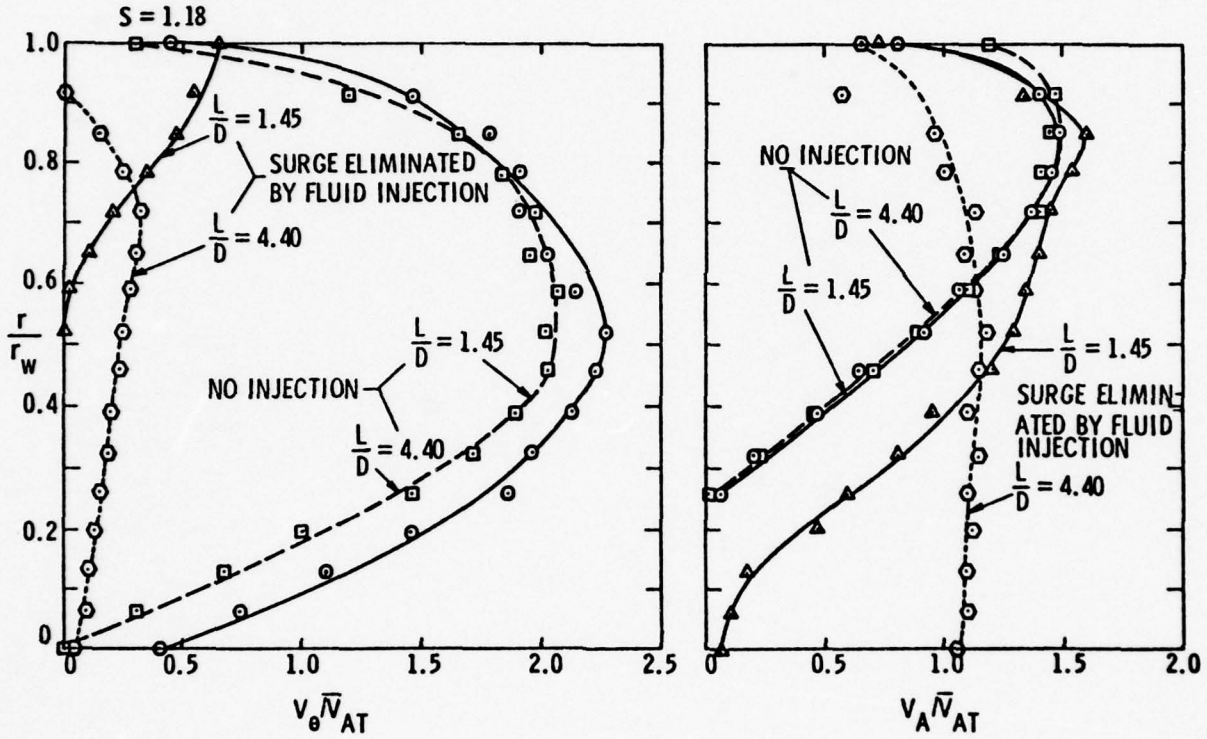

Figure 23. Mixing of injected flow with draft tube flow with respect to draft tube length.

CHAPTER V

COMPARISON OF TEST RESULTS WITH PREDICTIONS

5.1 Development of Empirical Relations

A relation to predict the ratio of bypass flow to turbine flow was previously derived and presented in Equation (15). This relation was developed assuming ideal momentum transfer between the injected fluid and the rotational flow in the draft tube. An empirical relation applicable to pump-turbines can also be derived using the experimental data presented in Figures 16 and 17. The bypass flow can be expressed as the product of the mass averaged velocity through the nozzle times the nozzle area or

$$Q_B = K_2(2gH)^{1/2}A_N \quad . \tag{21}$$

where K_2 is a nozzle coefficient that is assumed to have the value of 0.9. The flow rate through the turbine can be defined by the familiar power expression as

$$Q_T = \frac{1}{\eta}\frac{P}{H\gamma} \quad . \tag{22}$$

By combining Equations (21) and (22), an expression for flow ratio develops into

$$\frac{Q_B}{Q_T} = K_2\gamma(2g)^{1/2} \cdot \frac{\eta A_N H^{3/2}}{P} \quad , \tag{23}$$

where γ = 62.4 lb/ft^3 (1000 Kg/M^3), and g = 32.2 ft/sec^2 (9.81 m/sec^2).

Multiplying both numerator and denominator by A_T and substituting in the known values of given quantities, Equation (23) becomes:

$$\frac{Q_B}{Q_T} = 450.7\ \eta\ \frac{A_T}{P}\ \frac{A_N}{A_T}\ H^{3/2} \qquad \text{(English)} \tag{24}$$

or

$$\frac{Q_B}{Q_T} = \left[3987\ \eta\ \frac{A_T}{P}\ \frac{A_N}{A_T}\ H^{3/2}\right] \qquad \text{(Metric)} \quad .$$

With the experimental data shown in Figures 16 and 17, empirical relations to predict Q_B/Q_T as a function of A_N/A_T were developed for S = 1.18 and 0.80 and are plotted on the figures. The solid data points were selected for the simple linear regression of the two variables because these points represented nozzles that were circular or had an L/W ratio equal or close to 1.0. The other data points were not used in order to eliminate the effects of L/W ratio which were not detected in this study but could possibly still exist. For S = 1.18, a least squares fit of the data produced the relation

$$\frac{Q_B}{Q_T} = 0.719\left(\frac{A_N}{A_T}\right)^{0.401} , \tag{25}$$

and similarly, for S = 0.80:

$$\frac{Q_B}{Q_T} = 0.473\left(\frac{A_N}{A_T}\right)^{0.366} . \tag{26}$$

Equations (25) and (26) provide a convenient means of eliminating A_N/A_T from the right-hand side of Equation (24) for their respective swirl conditions. Therefore, if a swirl condition of S = 1.18 is considered, Equation (25) can be substituted into Equation (24) to give:

$$\frac{Q_B}{Q_T} = \frac{1}{103.7\left[\eta \frac{A_T H^{3/2}}{P}\right]^{0.669}} \tag{27}$$

$$= \left[\frac{1}{444.5\left[\eta \frac{A_T H^{3/2}}{P}\right]^{0.669}}\right] .$$

In a similar fashion, the substitution of Equation (26) into Equation (24) provides a relation of Q_B/Q_T for a swirl parameter of 0.80,

$$\frac{Q_B}{Q_T} = \frac{1}{110.9\left[\frac{\eta A_T H^{3/2}}{P}\right]^{0.577}} \tag{28}$$

$$= \left[\frac{1}{389.2\left[\frac{\eta A_T H^{3/2}}{P}\right]^{0.577}}\right]$$

Observation of Equations (27) and (28) shows that, given the geometric and performance data of a turbine installation, the required amount of bypass fluid to eliminate surge can be predicted for the surge conditions of S = 1.18 and 0.80.

Data similar to that shown in Figures 20 and 21 were also obtained with an elbow type draft tube in place of the cylindrical draft tube. The elbow type draft tube tested was similar to the Fontenelle configuration described by Palde [9]. Empirical relations were also developed for this data set and are shown in Figure 24, plotted with the data for S = 1.18 and 0.80. Using these empirical equations for the elbow type draft tube and Equation (24), relations similar to Equations (27) and (28) can be developed in likewise manner for the elbow type draft tube.

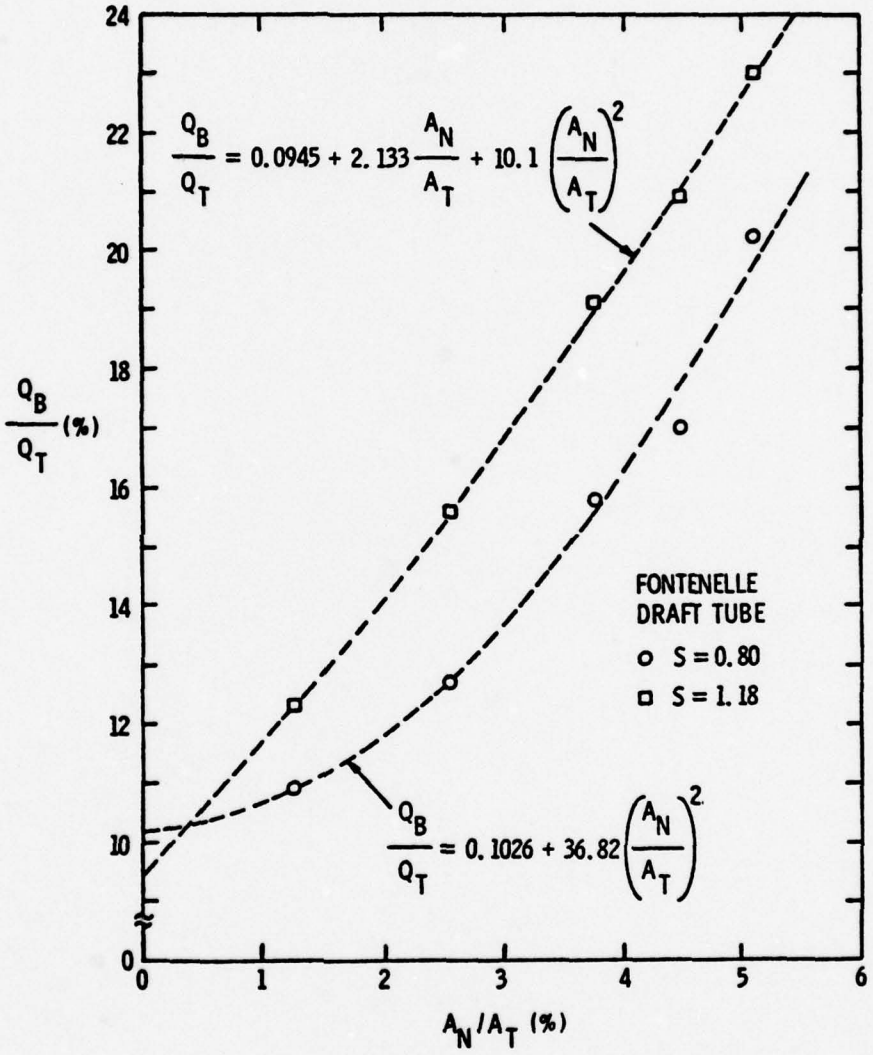

Figure 24. Injection flow required to eliminate surge using the Fontenelle (elbow type) draft tube.

5.2 Estimates of Bypass Flow for a Turbine Installation

In the report by Palde [10], geometric and performance data were given for the model of the Grand Coulee Third Power Plant Units. Therefore, the Grand Coulee Third Power Plant Units will be used as an example for the calculation of the bypass fluid required to eliminate surge. With the geometric and performance data, which are shown in Figure 25, the required bypass flow rates to eliminate surge in the turbine model for S = 1.18 and 0.80 can now be determined using Figure 21 and Equations (27) and (28), respectively. If we assume a speed coefficient ϕ_2 of 0.80, then the necessary performance data can be determined from Figure 25. Table II is a summary of the calculations necessary to predict Q_B/Q_T for swirl conditions of S = 1.18 and 0.80 using the empirical data. Calculations shown are for the cylindrical draft tube, although the results for the elbow draft tube are shown also. Table III shows the calculations required for solution of the theoretical relation, Equation (15), and Table IV is a comparative summary of the results of Tables II and III.

Table IV indicates that the empirically derived quantity of flow ratio required to eliminate surge at a swirl parameter of S = 1.18 is about 2.5 times greater than that predicted by assuming ideal momentum transfer.

The differences between the estimated empirical quantity and the estimated ideal quantity of Q_B/Q_T for S = 0.80 is smaller. The discrepancy between the ideal results and the empirical results is most likely due to poor assumptions made in the development of Equation (15). The assumption that ideal momentum transfer would occur in the test facility draft tube between the injection flow and rotational flow is probably not

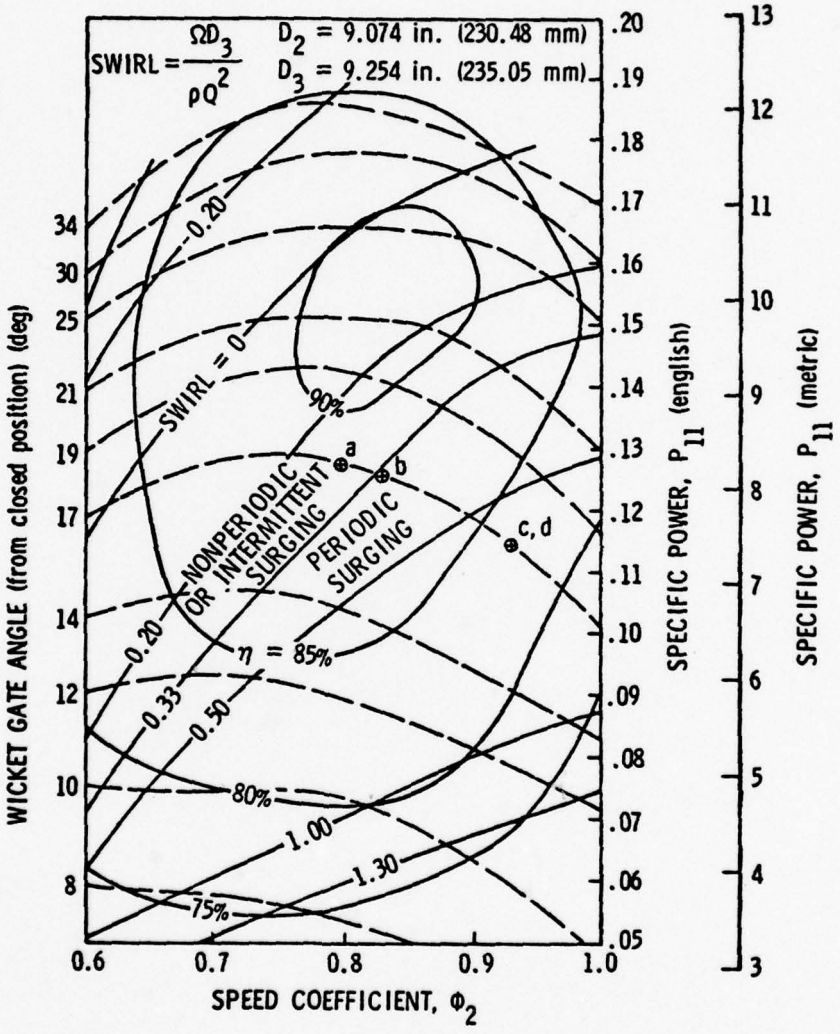

Figure 25. Performance and geometric data for the model of the Grand Coulee Third Power Plant Units.

TABLE II

Grand Coulee Third Power Plant, DEW 9" Model
(Reference Figure 25)
Empirical Prediction of Q_B/Q_T

$D_2 = 9.074$ in = 0.7562 ft (0.2305 m)

$D_3 = 9.254$ in = 0.7712 ft (0.2351 m)

$A = A_3 = 0.467$ ft^2 (0.0434 m^2)

Assumptions: $\phi_2 = 0.80$ = constant

$H = 320$ ft (97.5 m) = constant

$$P_{11} = \frac{P}{D_2^2 H^{3/2} 550} \; ; \; \frac{H^{3/2}}{P} = \frac{1}{D_2^2 P_{11} 550}$$

Swirl Parameter, S	Specific Power P_{11}	η	$\frac{H^{3/2}}{P}$	$\frac{Q_B}{Q_T}$
1.18	0.064	0.775	0.0497	0.1418
0.80	0.083	0.825	0.0383	0.1027

S = 1.18

$$\frac{Q_B}{Q_T} = \frac{1}{103.7 \left[\eta A_T \frac{H^{3/2}}{P}\right]^{0.069}}$$

S = 0.80

$$\frac{Q_B}{Q_T} = \frac{1}{110.9 \left[\eta A_T \frac{H^{3/2}}{P}\right]^{0.577}}$$

Fontenelle Draft Tube (Empirical Prediction)

Swirl Parameter, S	$\frac{Q_B}{Q_T}$
1.18	0.1319
0.80	0.1129

TABLE III

Grand Coulee Third Power Plant, DEW 9" Model
(Reference Figure 25)
Theoretical Prediction of Q_B/Q_T

$D_2 = 0.7562$ ft (0.2305 m)

$D_3 = 0.7712$ ft (0.2351 m)

$A_T = A_3 = 0.467$ ft^2 (0.0434 m^2)

Assumptions: $\phi = 0.80$ = constant
$H = 320$ ft (975 m) = constant
$S^* = 0.33$

$$Q_T = \frac{P_{11} D_2^2 H^{1/2} (550)}{\gamma \eta}$$

S	P_{11}	η	Q_T	$V_{A_T} = \frac{Q_T}{A_3}$	$\frac{Q_B}{Q_T}$
1.18	0.064	0.775	7.257	15.539	0.05605
0.80	0.083	0.825	9.114	19.516	0.06035
0.33 (S^*)	0.120	0.880	12.294	26.32 ($V_{A_T}^*$)	0

$$\frac{Q_B}{Q_T} = \frac{2.22 V_{A_T}^* \left[S \left(\frac{V_{A_T}}{V_{A_T}^*} \right) - S^* \left(\frac{V_{A_T}^*}{V_{A_T}} \right) \right]}{\sqrt{2gH}}$$

TABLE IV

Grand Coulee Third Power Plant Predicted Bypass Rates

	S = 0.80	S = 1.18
$\frac{Q_B}{Q_T}$, Predicted Ideal Equation (15) (%)	6.04	5.60
$\frac{Q_B}{Q_T}$, Predicted Empirically (%)	10.3	14.2 (cylindrical)
	11.3	13.0 (elbow)

valid. Therefore, the results of the empricial data should not be expected to match with the ideal data. Table IV also shows that the shape of the draft tube affects the efficiency of the injection process. More importantly, the rotational velocity profile in the draft tube was assumed to take the form of a potential vortex and the axial velocity distribution was assumed to be uniform. Figure 15 shows that the assumed velocity distributions were poor assumptions.

CHAPTER VI

SUMMARY AND CONCLUSIONS

The results of the experimental studies of injection nozzle geometries to implement the reduction of draft tube surge by fluid injection have led to the following observations:

1. Injection of high energy fluid counter to the rotational flow in the draft tube will reduce draft tube surge.

2. As the ratio of injected fluid Q_B/Q_T is increased, both the surge frequency and the magnitude of the surge amplitude decreases.

3. An angle of fluid injection up to 45^o does not affect the efficiency of the fluid injection scheme.

4. The use of various nozzle geometries with a fixed area ratio indicates no measurable change in the effectiveness of the nozzle with respect to eliminating surge.

5. For field installation, the selection of nozzle geometry shape would be primarily based on hydraulic efficiency and ease of fabrication.

6. Empirical data are presented which permit estimating the area of injection nozzles and the quantity of bleed fluid required for turbines of specified performance characteristics.

7. For a given swirl parameter, the bypass flow required to eliminate surge decreases as higher head turbines or lower specific speed units are considered.

CHAPTER VII

RECOMMENDATIONS

With the completion of this research on draft tube reduction, there emerges some areas of interest which require additional attention. The following is a list of recommendations for future investigation:

1. Appendix B shows the results of preliminary tests concerned with the effect of test apparatus geometry on the pressure amplitude of draft tube surge. The short study shows that a stilling chamber placed upstream or downstream of the wicket gate assembly has in most cases caused a reduction in surge pressure amplitude. Therefore, stilling chambers placed upstream or downstream of the turbine runner of a field installation may be an effective means of reducing draft tube surge. The geometry of the stilling chamber and its location relative to the turbine runner are probably important considerations. Further study is required in this area.

2. The theoretical Equation (15) derived in section 2.3 to predict the amount of bypass fluid required to eliminate a given surging condition has been proven to be a poor predicting equation by the results of section 5.2. Another approach to developing a predictive equation of required bypass rates should be investigated using more valid assumptions.

3. Table IV shows that the amount of bypass fluid required to eliminate a given surging condition is dependent upon the shape of the draft tube (the elbow and cylindrical shape are compared in Table IV). Further investigations are required to determine the influence of draft

tube shape on the reduction of surge by the injection of counterrotational fluid.

4. The hydrodynamic effects, such as cavitation, arising from the interaction of the draft tube flow with the high velocity injection jets should be experimentally investigated.

REFERENCES

1. Cassidy, J. J., "Experimental Study and Analysis of Draft-Tube Surging," Report No. REC-OCE-69-5, U. S. Bureau of Reclamation, Denver, Colorado, October 1969.

2. Cassidy, J. J. and H. T. Falvey, "Observations of Unsteady Flow Arising After Vortex Breakdown," Journal of Fluid Mechanics, Vol. 41, Part 4, pp. 727-736, 1970.

3. Dixon, S. L., Fluid Mechanics, Thermodynamics of Turbomachinery, 2nd Edition, Pergamon Press, New York, 1975.

4. Falvey, H. T. and J. J. Cassidy, "Frequency and Amplitude of Pressure Surges Generated by Swirling Flow," Transactions of Symposium Stockholm 1970, IAHR, Part 1, Paper E1, Stockholm, Sweden, 1970.

5. Falvey, H. T., "Draft Tube Surge--A Review of Present Knowledge and an Annotated Bibliography," Report No. REC-ERC-71-42, U. S. Bureau of Reclamation, Denver, Colorado, December 1971.

6. Gerich, R. and J. Raabe, "Measurement of the Unsteady and Cavity Flow in a Model Francis Turbine of High Specific Speed," ASME Journal of Fluids Engineering, December 1975, pp. 402-411.

7. Gubin, M. F., Draft Tubes of Hydro-Electric Stations, (Otsasyvayushchie Truby Gidroelektrostantsii), translated from Russian by Amerind Publishing, Co. Pvt. Ltd., New Delhi, 1973.

8. Murakami, Mitsukiyo, "Vibration of Water Turbine Draft Tubes," ASME Journal of Engineering for Power, January 1961, pp. 36-42.

9. Palde, Uldis J., "Influence of Draft Tube Shape on Surging Characteristics of Reaction Turbines," REC-ERC-72-24, U. S. Bureau of Reclamation, Denver, Colorado, July 1972.

10. Palde, Uldis J., "Model and Prototype Turbine Draft Tube Surge Analysis by the Swirl Momentum Method," IAHR and AIHR Symposium 1974, 1974.

11. Robertson, James M., Hydrodynamics in Theory and Application, Prentice-Hall Inc., Englewood Cliffs, New Jersey, 1965.

12. Rouse, Hunter, ed., Advanced Mechanics of Fluids, John Wiley and Sons, Inc., New York, 1959.

13. Ruud, F. O., "Vibration of Deriaz Pumps at Dos Amigos Pumping Plant," ASME Joint Fluids Engineering and Lubrication Conference, May 1975.

14. Rheingans, W. J., "Power Swings in Hydroelectric Power Plants," Transactions of the American Society of Mechanical Engineers, Vol. 62, 1940, pp. 171-184.

15. Shoop, Charles F. and George L. Tuve, Mechanical Engineering Practice, A Laboratory Reference Text, 3rd Edition, McGraw-Hill Book Company, Inc., New York and London, 1941.

16. Vennard, J. K., Elementary Fluid Mechanics, 4th Edition, John Wiley and Sons, Inc., New York, 1961.

17. Yocum, Adam, "Analysis of the Flow Through Turbine Wicket Gates with an Application to the Prediction of Draft Tube Surge," IAHR/ASME/ASCE Joint Symposium on Design and Operation of Fluid Machinery, Fort Collins, Colorado, June 12-14, 1978.

APPENDIX A

Dynamic Calibration of 1 psi Differential Data Sensors Pressure Transducer Performed by F. S. Archibald

During the course of the Draft Tube Surge Investigation, the question was raised about the dynamic sensitivity of the transducer being used. The static sensitivity of this transducer was found to be 0.0234 psi/volt, linear over the dynamic operating range. In order to investigate whether the dynamic sensitivity was different from the static sensitivity for frequencies up to 100 Hz, the transducer was calibrated twice, against a condenser microphone in both cases.

The frequency response of each Bruel and Kerr condenser microphone (1/2" and 1/4") was flat from ∿0 to 10 kHz, as evident from the individual calibration curves provided by the manufacturer. The sensitivity of each microphone (including amplifier system) was determined by using a piston phone calibrator.

In the two calibration situations to be described, a Spectral Dynamics Real Time Analyser (Model SD-301) was used in conjunction with a Spectral Dynamics Ensemble Averaging Unit (Model SD-302). The procedure was first to spectrally analyse the 250 Hz, 124 dB calibration signal from the microphone as produced by the piston phone calibrator to give an equivalent electrical spectral level. Subsequent spectral analyses of the microphone signal used this tone level from the calibration spectrum and accounted for analyser attenuator settings and system gains. Spectra of the subject transducer were calibrated using the inherent calibration of the spectrum analyser; i.e., input attenuator setting 0 dB reference is 100 mv. As this same analyser is used for all the experimental spectral data analysis, the machine internal calibration will be the same. However, the analyser electrical calibration has been checked by applying a known (as measured by a high quality voltmeter) RMS level sine wave. In the calibration situations to be described, the transducer was exposed to

the same pressure field as the microphone, and using the spectral analyser, the electrical output of the transducer was determined over the frequency range of interest. The transducer sensitivity can then be determined; i.e., S = P/$\overline{psi}$/Volt.

The two calibration situations used were a cavity of uniform (spatially) unsteady pressure and an unsteady pressure from a tapping in the Draft Tube Surge Apparatus. Figure 26 is a diagram of the pressure cavity showing the microphone and the transducer locations on the bottom of the cavity and the loudspeaker on the top. Since the highest frequency of interest is 100 Hz, which corresponds to an approximate 11-ft wave length, the cavity dimensions are much less than a wave length and the pressure will be uniform within the cavity. This presumes that the loudspeaker cone acts as a piston, an assumption that again ought to be satisfied for this small diameter speaker over the frequency range of interest. A white noise electrical signal (0-20 kHz) was applied to the loudspeaker at two levels, 5 and 0.5 Vrms. This resulted in an almost exact 20 dB difference in the pressure level over the 0-100 Hz range as measured by the microphone. It is noted that the lowest level was approximately 20 dB overall (linear weighting 2-40 kHz) above the noise background of the main bay area.

The spectral level of the pressure transducer signal also showed the same approximately 20 dB change over the frequency range between the two input white noise power levels, thus confirming response linearity with signal amplitude. Figure 27 compares spectra taken with the 1/2" microphone and pressure transducer. The frequency response of the pressure transducer appears quite flat, i.e., little difference between its spectral response and the microphone, known to be flat. Note that

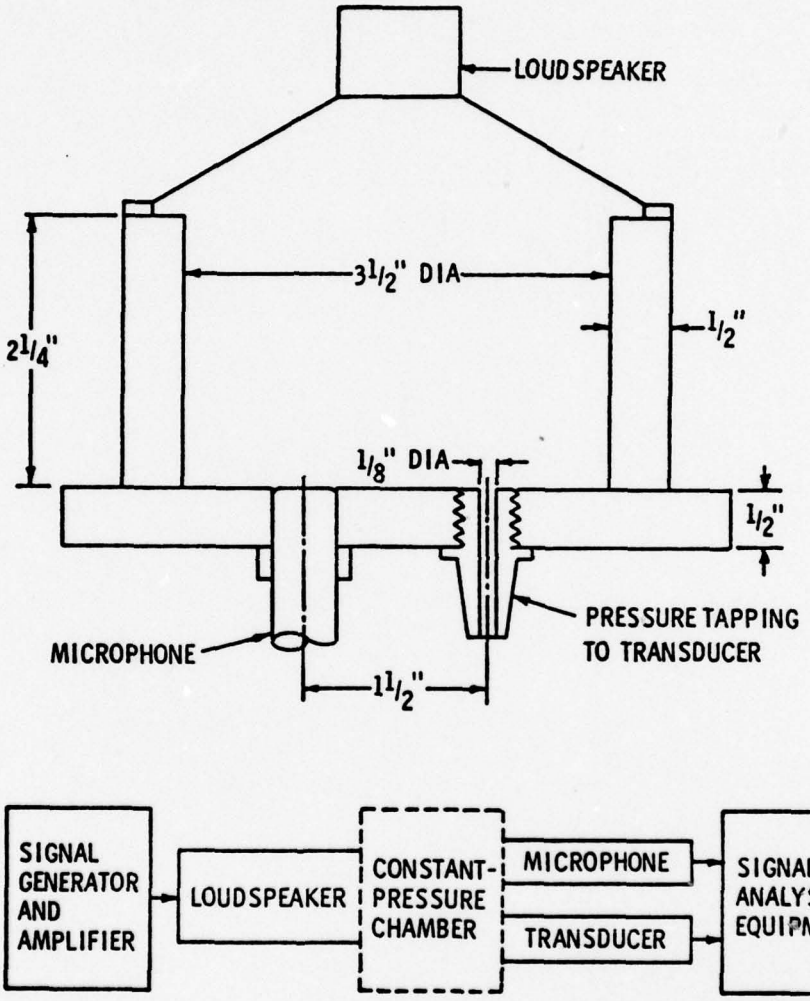

Figure 26. Schematic diagram of constant pressure calibration chamber showing location of microphone, pressure tapping, and loudspeaker.

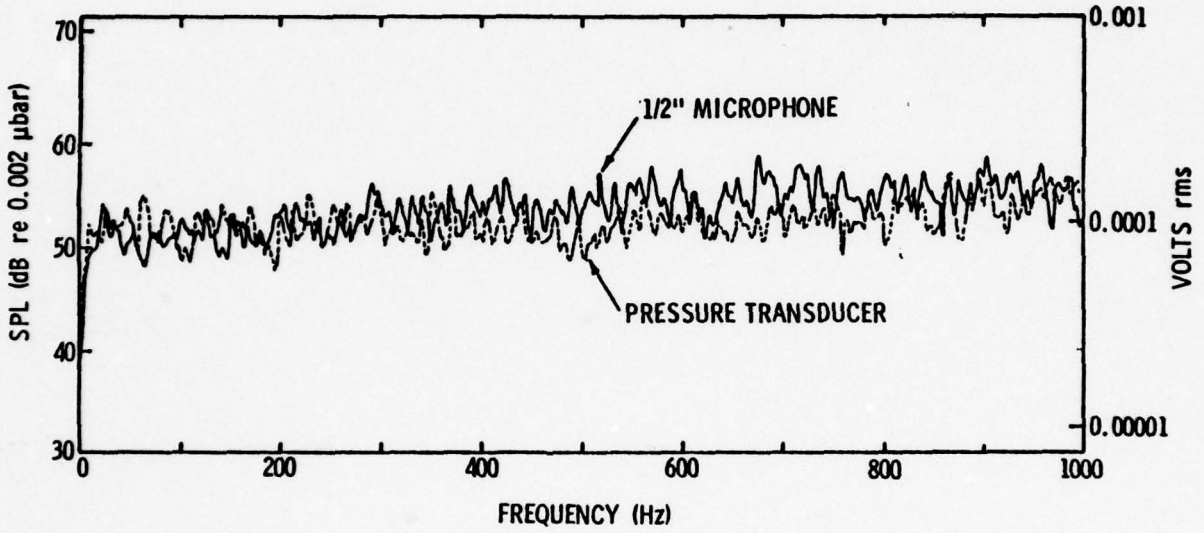

Figure 27. Spectral comparison of signals from 1/2" microphone and pressure transducer both simultaneously connected to constant pressure chamber with a white noise signal applied to the loudspeaker.

although the pressure in the cavity (as measured by the microphone) is not uniform with frequency, the deviations are approximately duplicated by the signal from the pressure transducer. It is possible to derive the frequency response of the pressure transducer by finding the difference in its response relative to the response measured by the microphone. For example, to find the transducer sensitivity, take the values at 30 Hz. The mean sound pressure level is 52 dB and the electrical level of the pressure transducer at this frequency is 0.0001 Vrms; therefore, S = 0.0117 psi/volt.

In order to dispel any doubt that the pressure transduced can accurately measure the pressure from a tapping in the research apparatus, a 1/4" microphone was connected with an approximately 2" long piece of 1/4" diameter plastic tubing. Figure 28 compares the spectra of the microphone and pressure transducer for the same operating condition, i.e., surge was strongly present. The spectra were overlayed to match the level at the top of the dominant "hat stack." Using the values at this frequency ($\sim$30 Hz), the sensitivity of the pressure transducer was computed to be 0.0265 psi/volt. This is in good agreement with the static sensitivity. In addition, it is seen that the pressure transducer signal agrees quite well with the signal from the microphone from 20 to 80 Hz.

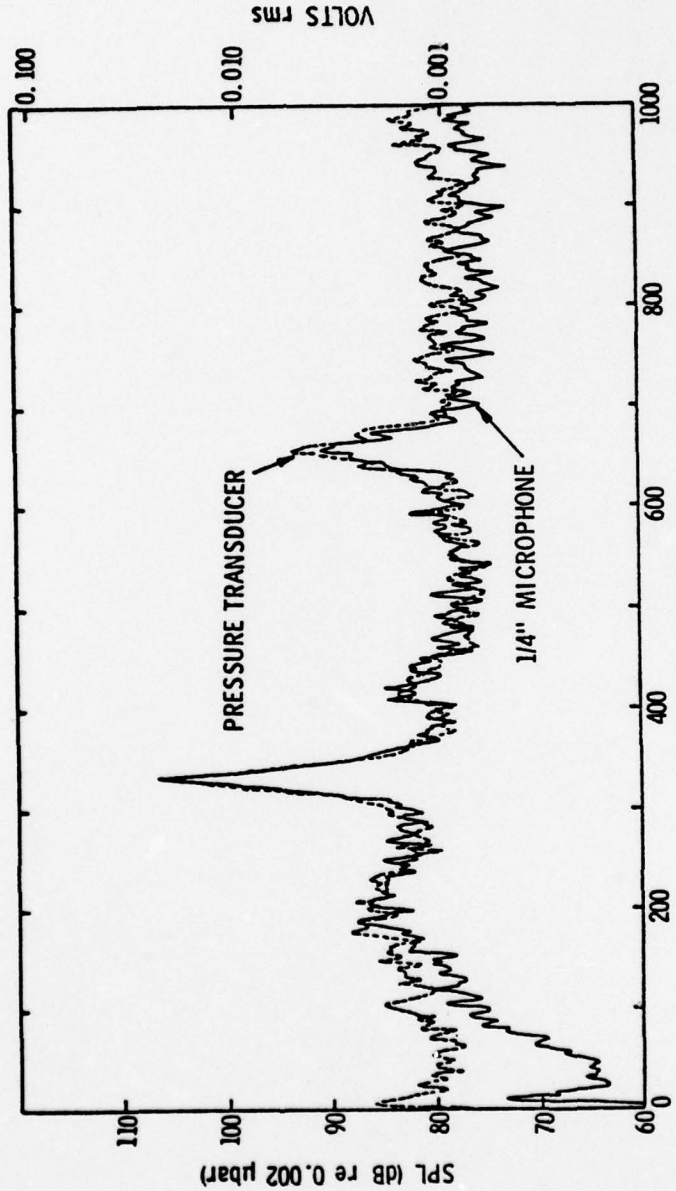

Figure 28. Spectral comparison of signals from 1/4" microphone and pressure transducer both alternately connected to a pressure tapping on the draft tube surge research apparatus operating with surge present.

APPENDIX B

Results of Preliminary Tests Indicating Effect of Test Apparatus Geometry on Surge Pressure

The test facility for the draft tube surge study as shown in Figure 7 was not the original test apparatus considered in the program. The original draft tube surge test facility was designed, fabricated, and assembled as shown in Figure 29. The main difference between the original test facility and the one finally used for testing is the location of the air supply flow fan. In the original test facility (Figure 29), air was drawn from the open atmosphere into the test section and dumped into a stilling chamber by means of a flow fan downstream of the draft tube. In the final test facility (Figure 7), air was blown into a stilling chamber first, then passed through the test section and dumped to atmosphere.

Examination of the sketches of the two facilities would seem to indicate that the important flow characteristics (pressure parameter and frequency parameter) produced in either test facility would be essentially the same. It was considered important for the test facility to produce relations between the surge parameters and the momentum parameter similar to those obtained by Palde [13]. Preliminary tests in the original test apparatus provided a relation between frequency parameter and momentum parameter much like that obtained by Palde. However, pressure parameter as a function of momentum parameter was essentially constant, which radically disagreed with Palde's data. In an attempt to obtain pressure parameter data similar to Palde's, various pressure pick-up devices were tried at various locations along the draft tube. After repeated failure to obtain the desired data in the original test facility, a test facility similar to that used by Palde (i.e., pushing air through the draft tube and dumping to atmosphere) was constructed as shown in Figure 7. Surging characteristics obtained in the modified test facility agreed very well with Palde's data. The altered test facility

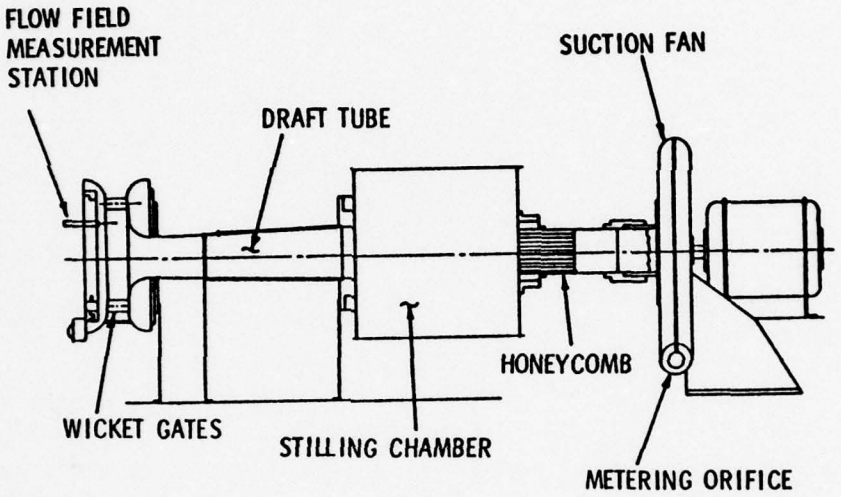

Figure 29. Schematic of the draft tube surge test facility originally designed and assembled.

solved the problem but raised a question. Why was the pressure parameter much lower for the original test facility compared to that obtained in Palde's or the final test facility? Velocity profiles obtained in the draft tube at L/D = 4.40 for each facility at various momentum parameters were compared. Figure 30 shows that the velocity profiles are quite similar for both test facilities.

In an effort to answer this question, a brief series of tests were performed to investigate the effects on pressure parameter of dumping the draft tube flow into a stilling chamber and then dumping to atmosphere. Tests were performed on both the cylindrical and elbow type draft tubes. Tables B1 and B2 show the different geometries that were investigated. With any given facility geometry tested, a survey of pressure parameter as a function of momentum parameter was obtained. The flow rate through the test facility was measured by an orifice meter and the surge pressure was measured through a dynamically calibrated pressure transducer by an RMS meter as earlier described in this report.

Figure 31 shows the results of this investigation for the cylindrical draft tube and likewise Figure 32 corresponds to the Fontenelle (elbow type) draft tube. The numbers on the curves in Figures 31 and 32 correspond to the geometries so numbered in Tables B1 and B2. Comparison of curves (1) and (2) in Figure 31 shows the effects of a stilling chamber below the draft tube on pressure parameter. Looking at all the curves of both Figures 31 and 32, it is obvious that the use of the stilling chamber in all cases reduced the pressure parameter magnitude. Notice that screens placed across the stilling chamber /curve (5), Figure 31/ forced the pressure parameter relation of the original test facility to become almost identical to those of Palde and curve (2).

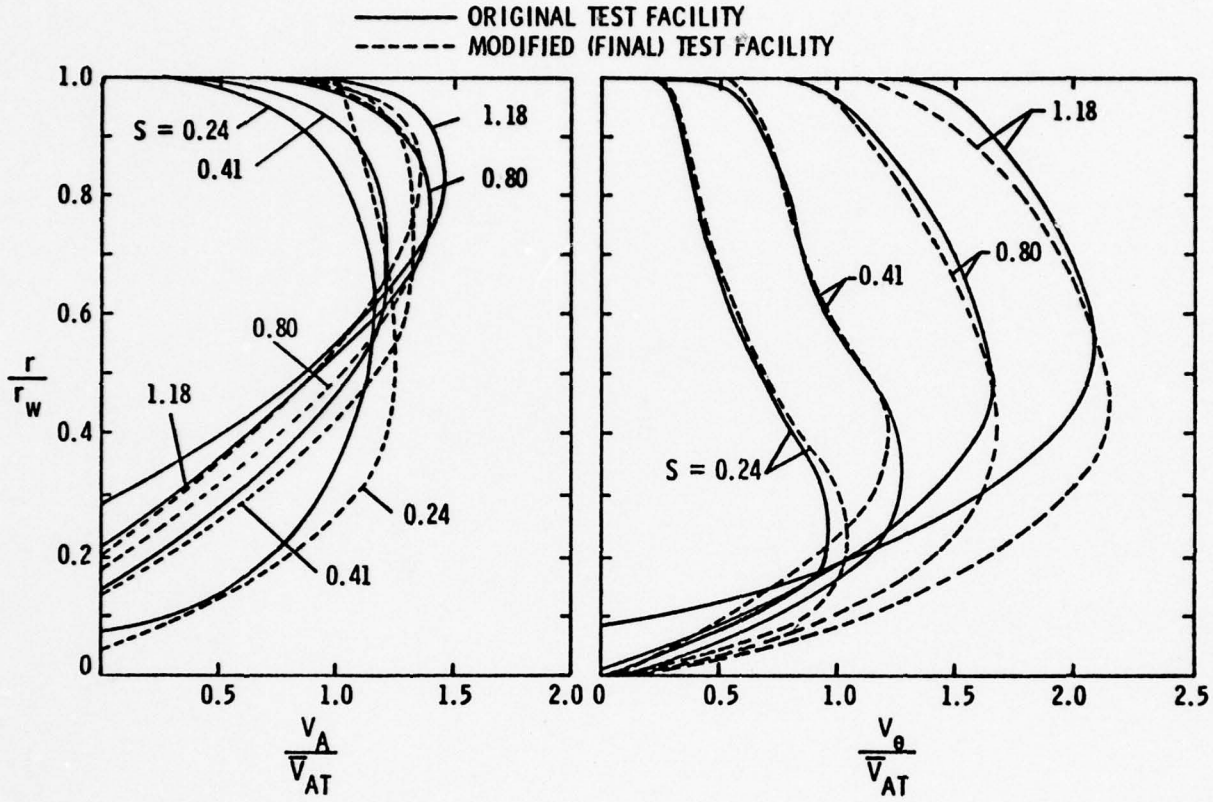

Figure 30. Comparison of velocity profiles of the two test facilities for various swirl parameters.

TABLE B1

TEST APPARATUS GEOMETRIES INVESTIGATED WITH RESPECT TO SURGING CHARACTERISTICS USING THE CYLINDRICAL DRAFT TUBE

1. STILLING CHAMBER AND AIR SUPPLY DOWNSTREAM OF DRAFT TUBE

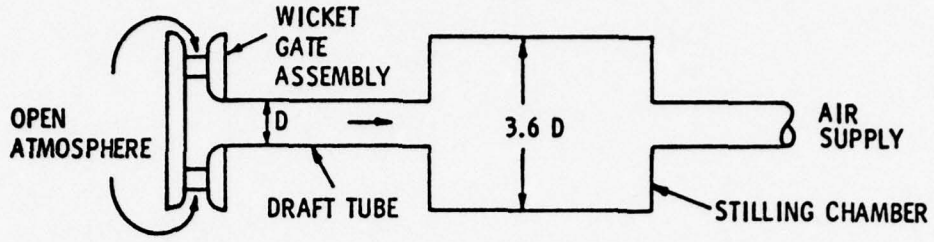

2. NO STILLING CHAMBER, UPSTREAM AIR SUPPLY

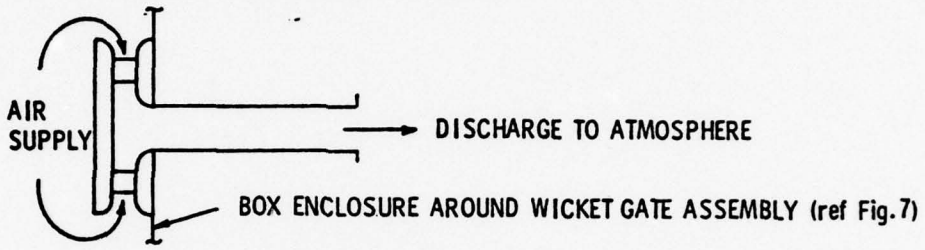

3. STILLING CHAMBER DOWNSTREAM OF DRAFT TUBE, UPSTREAM AIR SUPPLY

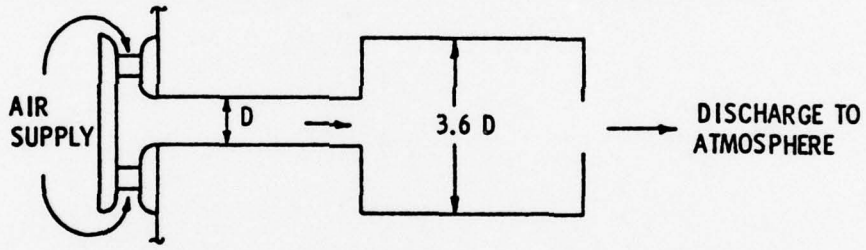

4. STILLING CHAMBER AND AIR SUPPLY UPSTREAM OF DRAFT TUBE

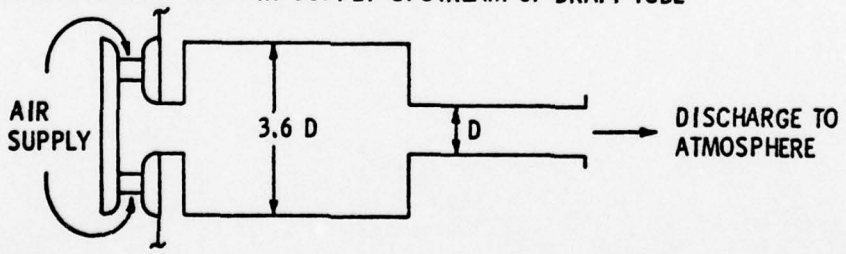

5. STILLING CHAMBER WITH SCREEN DOWNSTREAM OF DRAFT TUBE, UPSTREAM AIR SUPPLY

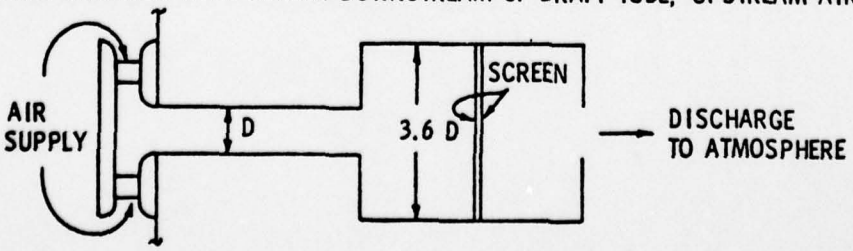

TABLE B2

TEST APPARATUS GEOMETRY INVESTIGATED WITH RESPECT TO SURGING CHARACTERISTICS USING THE ELBOW TYPE DRAFT TUBE

1. NO STILLING CHAMBER, UPSTREAM AIR SUPPLY

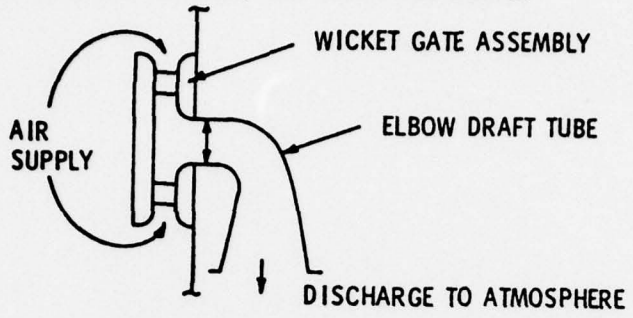

2. STILLING CHAMBER DOWNSTREAM OF DRAFT TUBE, UPSTREAM AIR SUPPLY

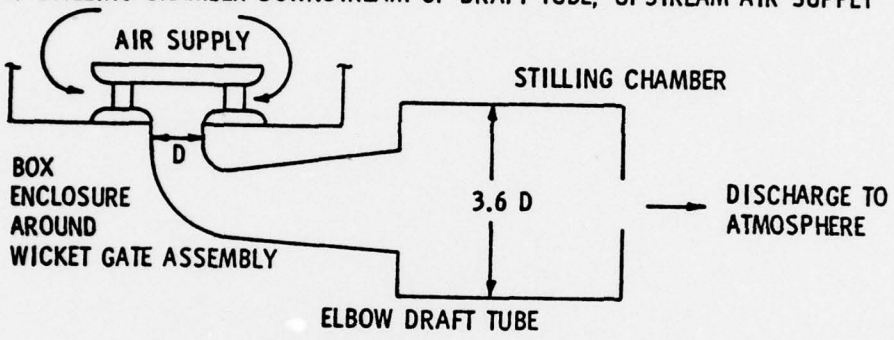

3. STILLING CHAMBER (SHORT CONNECTION) UPSTREAM OF DRAFT TUBE, UPSTREAM AIR SUPPLY

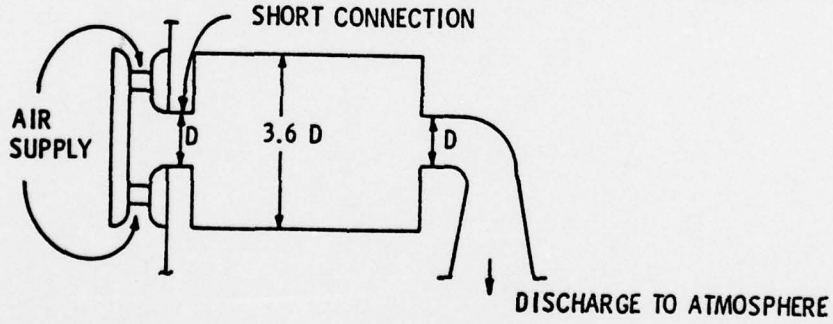

4. STILLING CHAMBER (LONG CONNECTION) UPSTREAM OF DRAFT TUBE, UPSTREAM AIR SUPPLY

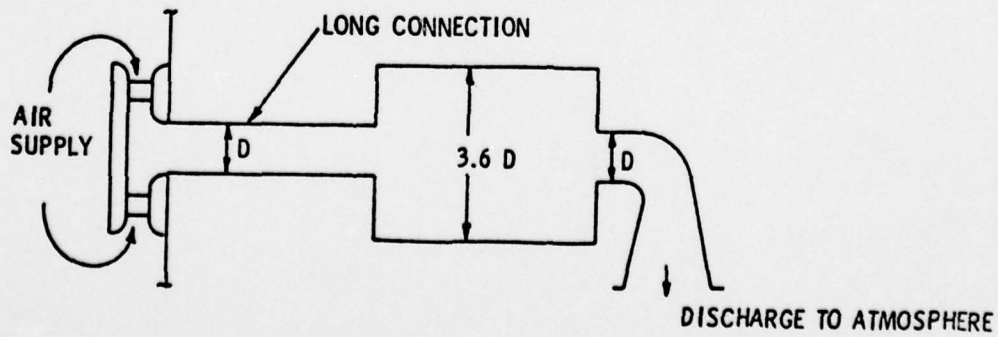

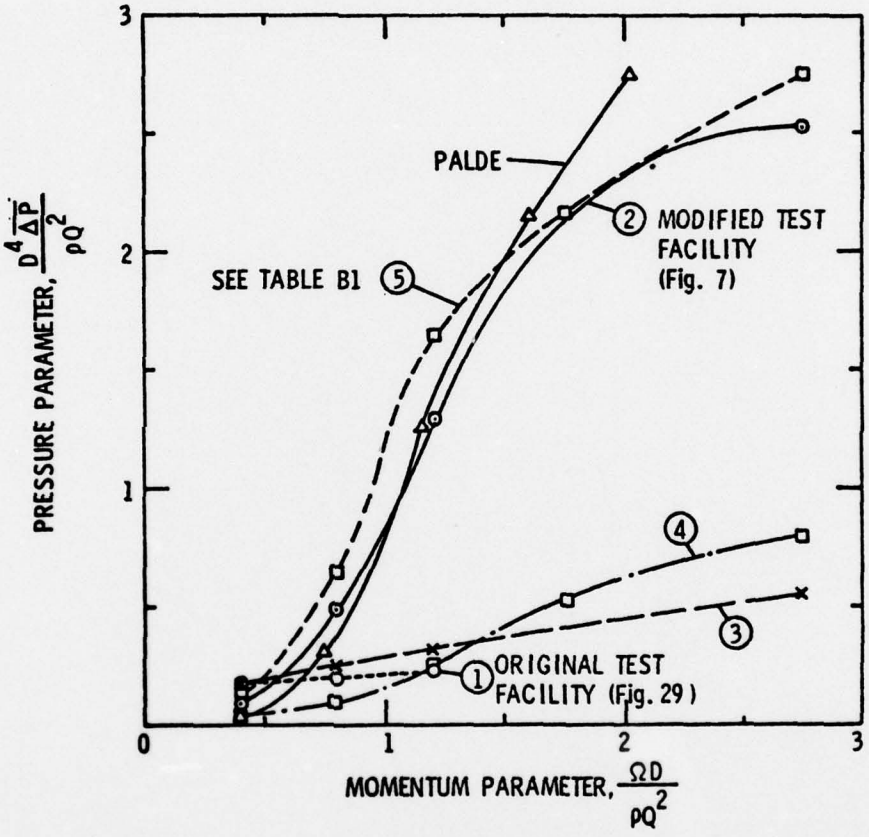

Figure 31. The effect of test apparatus geometry on pressure parameter using the cylindrical draft tube.

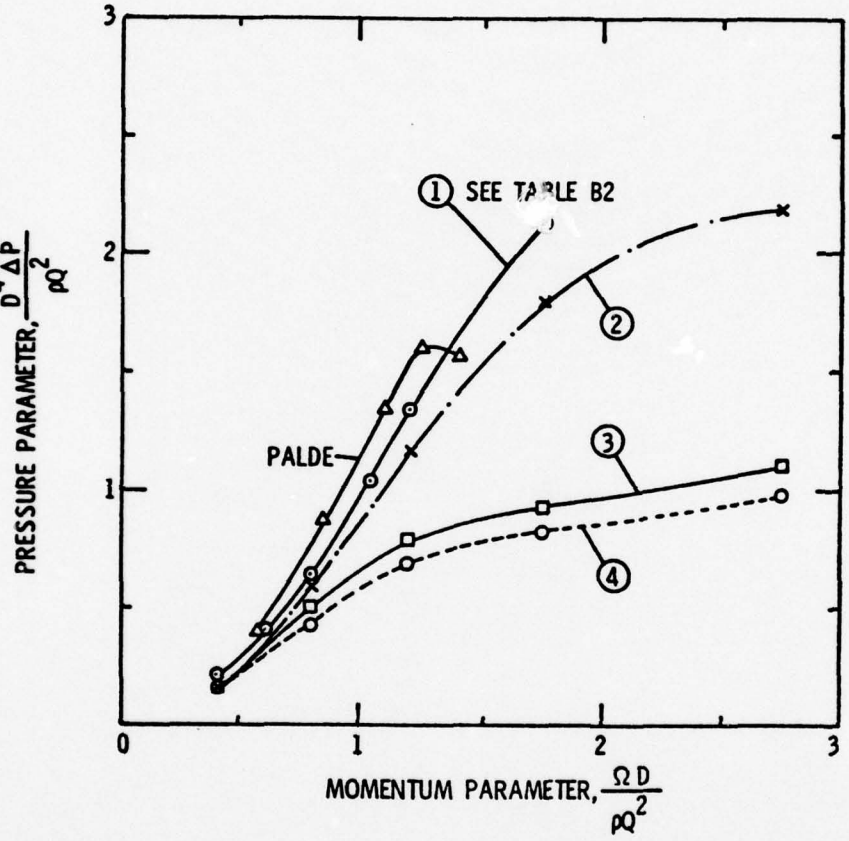

Figure 32. The effect of test apparatus geometry on pressure parameter using the elbow type draft tube.

Out of this brief study comes speculation that stilling chambers placed downstream of a turbine runner may be an effective means of reducing draft tube surge in hydroelectric pump-turbines. Further study is required in this area.

A second implication has been suggested by H. Falvey of The Bureau of Reclamation. This involves the geometry of model test loops which have stilling chambers located up or downstream of model pump-turbines. The water level and geometry of these chambers could provide surge characteristics, based on model tests, that are inconsistent with those of the prototype.

DISTRIBUTION

Commander (NSEA 09G32)
Naval Sea Systems Command
Department of the Navy
Washington, D. C. 20362 — Copies 1 and 2

Commander (NSEA 0342)
Naval Sea Systems Command
Department of the Navy
Washington, D. C. 20362 — Copies 3 and 4

Defense Documentation Center
5010 Cameron Street
Cameron Station
Alexandria, VA 22314 — Copies 5 through 16